2017

A Magnetic Resonance Compatible Knee Extension Ergometer

Youssef Jaber
University of Massachusetts Amherst

A MAGNETIC RESONANCE COMPATIBLE KNEE EXTENSION ERGOMETER

A Thesis Presented

by

YOUSSEF JABER

Submitted to the Graduated School of the

University of Massachusetts Amherst in partial fulfillment

of the requirements for the degree of

MASTER OF SCIENCE IN MECHANICAL ENGINEERING

May 2017

Mechanical and Industrial Engineering

A MAGNETIC RESONANCE COMPATIBLE KNEE EXTENSION ERGOMETER

A Thesis Presented

by

YOUSSEF JABER

Approved as to style and content by:

_____

Frank C. Sup IV, Chair

_____

Jane A. Kent

_____

James R. Rinderle

_____

Sundar Krishnamurty, Department Head
Mechanical and Industrial Engineering

ABSTRACT

A MAGNETIC RESONANCE COMPATIBLE KNEE EXTENSION ERGOMETER

MAY 2017

YOUSSEF JABER

B.S.M.E, JORDAN UNIVERSITY OF SCIENCE AND TECHNOLOGY, IRBID, JORDAN

M.S.M.E, UNIVERSITY OF MASSACHUSETTS, AMHERST

Directed by: PROFESSOR FRANK C. SUP IV

The product of this thesis aims to enable the study of the biochemical and physical dynamics of the lower limbs at high levels of muscle tension and fast contraction speeds. This is accomplished in part by a magnetic resonance (MR) compatible ergometer designed to apply a load as a torque of up to 420 Nm acting against knee extension at speeds as high as 4.7 rad/s. The system can also be adapted to apply the load as a force of up to 1200 N acting against full leg extension. The ergometer is designed to enable the use of magnetic resonance spectroscopy and imaging in a three Tesla Siemens Skyra MRI system. Due to the electromagnetic limitations of having the device operate inside the magnet, the design is split into two components. One designed to fit inside the 70 cm bore of the scanner. This component is electromagnetically passive; made out of materials exhibiting minimal magnetic interference, and having no electrically powered parts. The other component is electromagnetically active; it contains all of the powered elements and actuates the passive part from another room. A tensioned cable transmits power through a waveguide; a pipe through the wall of the MRI room with an RF shield. The device was tested applying a sagittal plane moment on the knee joint during isometric, isokinetic, isotonic, and constant power contractions. The mean percent error relative to the reference was less than 9% in isotonic, 2% in isokinetic, and 10% in constant power mode, and the stiffness of the controller in isometric mode was about 1500 Nm/deg.

TABLE OF CONTENTS

Page

LIST OF TABLES

Table Page

LIST OF FIGURES

CHAPTER 1

INTRODUCTION

1.1 Problem Statement

Using magnetic resonance imaging (MRI) along with magnetic resonance spectroscopy (MRS) enables accurate noninvasive metabolic energy measurements of active muscles and the characterization of the tissue. However, for such a technique to be used on an exercising muscle, a magnetic resonance compatible ergometer targeting those muscles at the target power levels needed to be developed. MR-compatible design accounts for the presence of the strong electromagnetic fields generated by the scanner. That includes both the effect of the field on the device to be designed regarding safety and functionality and the effect of the designed device on the field, which can lower the scanning quality. This interaction between the scanner and other devices close to its fields is called mutual interference [1], and the goal of an MR-compatible design is to limit it to a point where the device achieves the desired performance safely without greatly affecting the scanning quality.

1.2 Objective

The goal of this project is to design a magnetic resonance compatible ergometer to target the quadriceps femoris muscle group in the lower limb, enabling the study of its tissue while the muscles are near their physical workload limits. This is done by applying a controlled resistive load to allow for both static and dynamic muscle contractions. Further, the device should follow good human factor practices and be easy to setup, operate, and provide the user with data.

1.3 Project Overview

This thesis describes the design of a magnetic resonance compatible ergometer that enables the use of magnetic resonance spectroscopy and imaging of the lower limb as it is exercised against a controlled resistive load. The device is capable of controlling its applied load

to stimulate multiple types of muscle contractions: Isometric (where the load is applied to resist motion), Isotonic (where the load is constant through the contraction), Isokinetic (where the load is varied to limit the velocity to a set value), and constant power (where the relation between load and velocity is controlled to maintain a constant power output).

Multiple MR-compatible ergometers have been previously developed; many were designed for static load application, allowing for isometric muscle contractions only. Most MR-compatible ergometers capable of stimulating dynamic contractions applied the load passively, with no feedback control. Among the ergometers that did have active control, none were designed to stimulate more than two types of muscle contraction.

This ergometer described in this work achieves MR compatibility by locating all the powered actuation and sensing elements away from the field and having them placed in an adjacent room. Those elements are connected mechanically using cable and a system of pulleys to passive components inside the scanner bore. This separation removes many of the constraints of the magnetic fields on actuator and sensor selection. The ergometer uses an AC servo motor to apply its load to meet the high workload requirements that match the lower limb of an exercising human. A back drivable ball screw is used with the motor, translating its rotational motion into a linear motion, and amplifying its load.

The device is controlled through a user interface running on a computer in a separate room. The interface allows for simple test protocol setup, real-time data monitoring and logging, and automatic data analysis. An MR-compatible fiber optic monitor is also connected to the interface and can be seen by the test participant using the ergometer. The fiber optic monitor provides real-time visual feedback to the user. The monitor is used to display a 2D trace of the user's performance compared to a target they are asked to hit. Auditory feedback is also provided to help sync the end of the contraction with the magnetic resonance scan cycle.

1.4 Organization

This thesis starts with an introduction, which includes the problem statement, the objective, and the organization of the study. Next is the background, starting with a basic introduction to magnetic resonance imaging and spectroscopy, moving onto an overview of MR-compatible design considerations and ending with a review of related prior work. The system design chapter covers the approach used to identify the design requirements, then goes over the mechanical system design, followed by a section describing the system architecture. The fifth chapter starts with signal processing and follows that with the controller specifications for the position, velocity and torque controllers. The chapter ends with a description of the finite state machine controllers for isometric, isotonic, isokinetic and constant power modes. The test methodology, data, and analysis are in the results chapter. The thesis ends with the conclusion, which includes a summary of the presented work followed by some suggested applications.

CHAPTER 2

BACKGROUND

2.1 Magnetic Resonance Imaging and Spectroscopy

A magnetic resonance machine works by producing a very strong magnetic field using a superconducting coil cooled by liquid helium. The helium circulates in the coil at a temperature of about 4 Kelvin lowering the resistance of the coil and allowing very high currents to pass through. The process used to take a scan is shown in Figure 1. The static field produced by the current aligns the spin of the hydrogen protons inside the bore with the magnetic field. About half of the protons will line up with the magnet in one way (south to north and north to south) while the rest line up the other way (south to south and north to north). Most of the protons match with other protons with the opposite spin, but very few are left out without a match. While in this configuration, another coil called the RF coil produces a wave that resonates with the protons that did not match. The protons flip to a high energy configuration, then when the RF wave passes they flip back and produce a pulse [2].

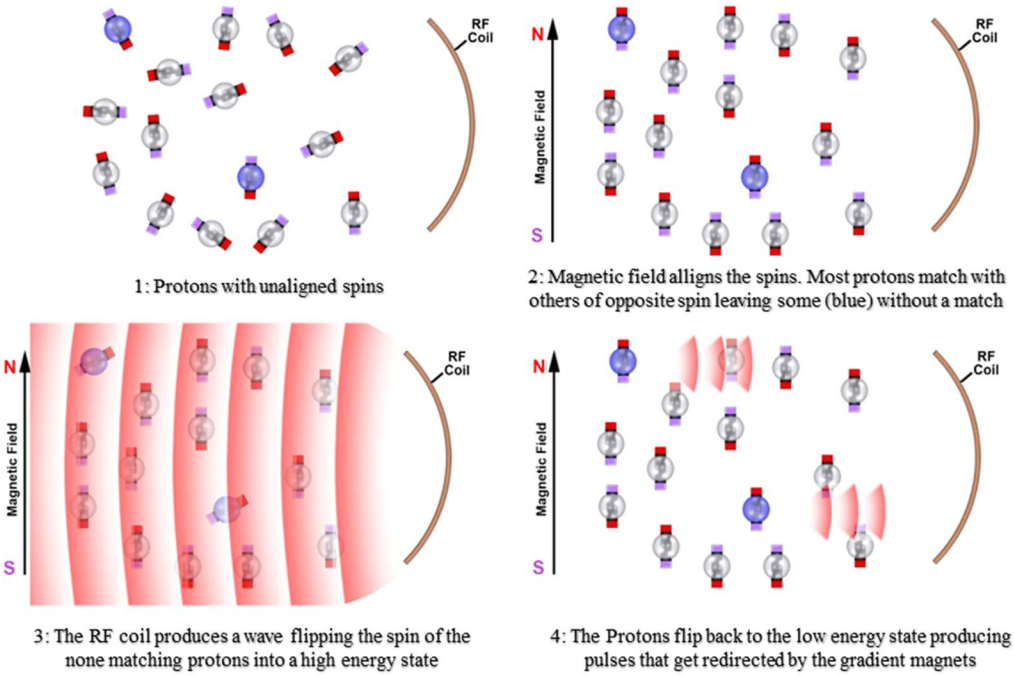

Figure 1: Process of Magnetic Resonance Imaging [2]

Through each different scan cycle, three other magnets called the gradient magnets would be turned on and off at specific times relative to the RF coil pulses. With that, the spatial characteristics of the magnetic resonance scan can be varied to specify the orientation of the slice plane [3].

An MRI machine is designed to target and detect protons of hydrogen atoms in a water molecule, protons of other atoms or hydrogen atoms in other molecules are not detected. Magnetic resonance spectroscopy (or MRS) makes use of spectroscopy coils with a broader range of spatial resolution to detect the intensity of other atoms, like phosphorus, carbon or hydrogen (not necessary in water molecules) this enables accurate none invasive measurements of biochemical changes in the body [4]. An example of a spectrum captured using MRS in a three Tesla scanner is shown in Figure 2:

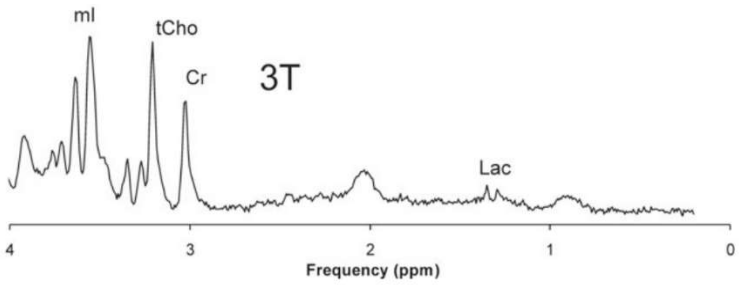

Figure 2: Spectrum captured using MRS

2.2 Designing for MR Compatibility

The main concern when it comes to MR-compatible design, in general, is the presence of strong electromagnetic fields produced by the scanner. Design conditions were proposed to help the process of developing new MR-compatible devices [1, 5, 6, 7]. Compatibility in terms of safety, the effect on the scanning quality, and device performance need to be also taken into account.

2.2.1 Safety Considerations

The magnetic force produced along with heat generation are some of the principal safety concerns. Magnets and ferromagnetic materials are affected by the static magnetic field as it

exerts a force on them, turning parts made of those materials into potentially dangerous projectiles [8, 9]. Thus, the use of such materials in parts inside or near the MRI machine must be avoided. In cases where the use of ferromagnetic materials is necessary, and should they be placed away from the isocenter, those parts can be restrained in place [1]. The forces acting on the ferromagnetic parts can be calculated either by hand or using finite element analysis software. The structure holding the ferromagnetic parts in place needs to be designed to withstand the calculated loading conditions.

The dynamic field produced by the RF coil can induce a current in loops made out of conductive materials; the static field can also induce a current if a conductive loop moved through it, those loops would act as heating elements causing burn injuries if they were near the body [10]. The heat generated is proportional to the area enclosed by the loop, the conductivity of the materials used, and in the case of a moving loop, the speed at which it is moving among other factors. Therefore, large conductive loops near the body should also be avoided. The length of conductive elements is another criterion to be taken into account. If the conductive part had a length close to a multiple of the half-wavelength of the RF field, it could also heat up as it resonates with the field. The RF wavelength in a conducting element depends on the strength of the field (which relates to the nominal frequency) and the dielectric constant of the material surrounding the conductive part. The following equation can be used to calculate it:

$$\lambda = \frac{c}{f\sqrt{\epsilon}} \qquad (1)$$

$Where\ \lambda: Wavelength, c: Speed\ of\ light, f: Nominal\ frequency, and\ \epsilon: dielectric\ constant$

For a three Tesla scanner (nominal frequency = 128Mhz) and a part surrounded by water ($\epsilon = 81$) for example, the wavelength would be 0.26 meters. Therefore, a conducting part close to the body with a length that is a multiple of 13 centimeters in this case would resonate and heat up as the RF coil produces a pulse of that frequency.

2.2.2 Limiting Effect on Scanning Quality

Conductive loops can distort the field affecting scanning quality; this is due to the magnetic field generated by the induced current. Therefore, even if the loops are not close to the body or if the heat generated is not a problem, the effect on scanning quality could be significant. Ferromagnetic parts can also cause distortions in the field, even if they are restrained in place. Restraining them away from the scanner can limit their effect and designs that use such materials can be implemented with little impact on the scanning quality [1]. Avoiding their use altogether is a safer option. Other than conductivity and ferromagnetism, the magnetic susceptibility of the materials is another factor to be looked into [11]. The magnetism of materials can either be inherent or induced, and the magnetic susceptibility is a measure of the level of magnetization of a material induced by an applied magnetic field. This too can have an effect on the scanning quality, and so it should be a factor in the material selection process. Materials with a magnetic susceptibility in the order of $\pm 10^{-5}$ are considered MR safe. A positive magnetic susceptibility value indicates that the material is paramagnetic while a negative value means that it is diamagnetic. With a magnetic susceptibility ranging from 3.52×10^{-3} to 6.7×10^{-3}, stainless steel is an example of a material that is not necessarily magnetic but can cause problems due to its magnetic susceptibility. Table 1 lists the susceptibility of a few materials that are within the safe range of MR-compatibility.

Material	Water	Copper	Aluminum	Silica	Pyrex Glass	Magnesium
Susceptibility ($\times 10^{-6}$)	-9.05	-9.63	20.7	-16.3	-13.88	11.7

Table 1: Magnetic Susceptibility of Some Materials

2.2.3 Limitations on Powered Components

The choice of using powered actuators and electromechanical sensors is limited due to their effect on image quality and the field's effect on their functionality. Shielding those elements and their connectors can limit the problem. Some designs place all of the powered components of

the device in a Faraday cage to help reduce mutual interference [12, 13], but that is not a practical solution in most cases.

The use of light-based sensors is very common in MR-compatible designs. Optical encoders used to measure velocity or position are implemented in some designs [14, 15]. The encoders work by transmitting light to the MRI machine and back using fiber optic cables. That way, the powered light sources, and transducers are kept at a distance. Light-based force sensors have also been developed [16,17,18]. Figure 3 shows an example of a light based force sensor. Those sensors use small structures that deform elastically when a load is applied. Light is transmitted into, and back from those structures via fiber optic cables, and the amount of light that gets back changes based on how deformed the structure is. In Figure 3, the distance, h, changes when a load is applied, and as a result more of the light gets defused away from the receiving cable changing the sensor reading.

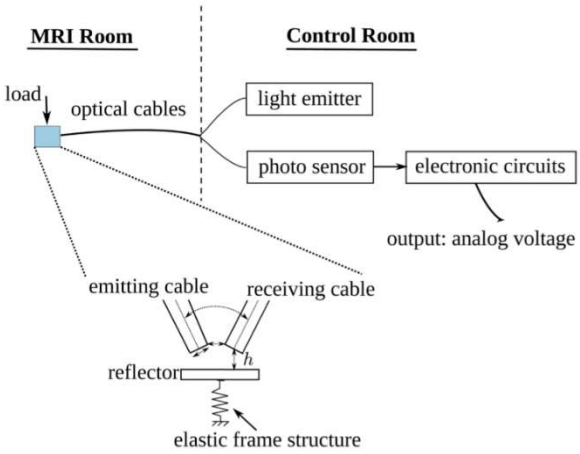

Figure 3: Fiber Optic Force Sensor

For actuation, ultrasonic piezoelectric actuators are commonly used when precise direct control is required [14, 19, 20] those actuators are not powerful enough for some applications. Therefore, hydraulic and pneumatic actuators are used in some of those cases [21, 22]. Other designs make use of mechanisms like a Cardan or linkage system to transmit power from a conventional actuator away from the field into the MRI machine [23, 24].

2.2.4 Human Factor, Ergonomics, and Mechanical Design Requirements

Other design requirements not related to the electromagnetic field come from the specifics of the device usage and the physical specifications of the scanner used. Most MRI machines incorporate a closed bore design. The shape and dimensions of the bore are design constraints if the device is to be used within it. The components meant to be inside should be designed to fit, to be easily installed, and locked in place without damaging the scanner. Human factors and ergonomics add another set of design requirements. The components interfacing between the user and the device should be comfortable and safe to use for all of their intended users. The structural and dynamic properties of the design and the materials used is another set of design requirements that depend on the anticipated loads the device will be subjected to. Finite element analysis along with simulations of the device can be used to check the structural stability of the design or to optimize design parameters.

2.3 Prior Work: MR-compatible Exercise Apparatus

Many MR-compatible ergometers have been developed, most of which only allowed the user to perform isometric contractions [25, 26]. Such designs are simple to implement. However, since the force is applied on a stationary part capable of only measuring the load applied, there will be no physical work done, and no mean to mechanically quantify the energy used by the muscles. This section will focus on dynamic exercise apparatus capable of measuring the work done.

2.3.1 Passive Designs

An ergometer developed by Francescato et el. [27], is capable of measuring the angular position and the force produced by the calf muscle over the range of a contraction. This design is shown in Figure 4. A force transducer (strain gauge) is used to measure the force and a potentiometer to measure the position. The load applied is produced by elastic cords pre-stretched to work in their linear region, the number of cords can be changed to vary the load, and at a very

high limit, the user will be effectively doing an isometric contraction. The power applied through the range of motion should be constant here. Moreover, the range of motion can be changed by sliding a stop block. However, since the resistive load applied depends on the position, the torque could not be constant through the contraction in this design. Hence, this ergometer will not allow for isotonic contractions.

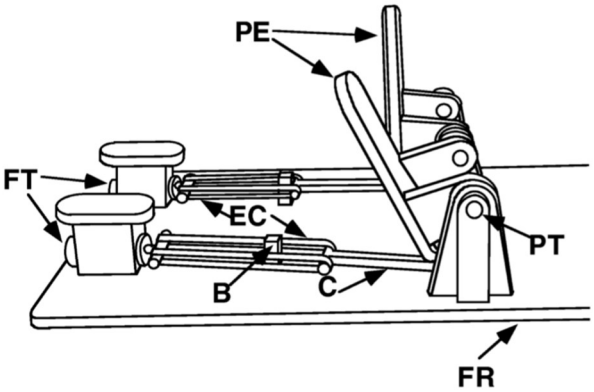

FR=Wooden Frame, PE=Pedals, C=non-elastic nylon cable,
EC=elastic cords, B=Stop block, PT=Potentiometer,

Figure 4: Ergometer Implementing Elastic Cords

Another design shown in Figure 5 maintains constant load through the contraction. It makes use of a combined hydraulic - pneumatic system [28], this system also targets the calf muscles. It measures the ankle joint angle using a potentiometer and assumes the force to be related to the set pneumatic pressure. The mechanism consists of a small hydraulic cylinder attached to the pedal and connected through a tube and a valve to a larger cylinder. An air tank provides regulated pneumatic pressure to the larger cylinder; this pressure is transferred hydraulically onto the smaller cylinder which applies it as a force pushing against the pedal.

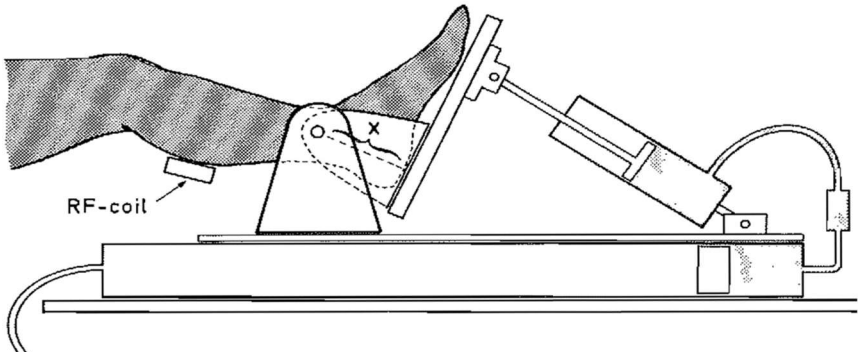

Figure 5: Combined Hydraulic-Pneumatic MR-Compatible Ergometer

The main problem with this design is the limitation on speed. At high speeds, friction becomes significant, and the system starts acting as a damper. The researchers use a choke valve between the two hydraulic cylinders to limit the speed and mitigate this problem. However, this can deteriorate the performance of the ergometer at lower speeds. Another issue is the changing angle between the small cylinder and the pedal. That angle will influence the effective torque applied to the calf muscle through the contraction; The torque will decrease the further away the angle is from being perpendicular to the displacement vector (the vector connects the point of contact to the joint).

Designs are plentiful where the load is produced by hanging weights connected to the leg of the user either directly or through a mechanism [29, 30, 31]. They can provide set load values at constant speeds, but that load changes as the weights are accelerated to meet the required speed and towards the end of each contraction where the speed drops. So only the constant speed regions of the contraction can be considered isotonic. The load is also applied during the eccentric part of the contraction which is not desired in some cases. Additionally, the designs have the same problem with the changing angle between the force and the displacement vector, which should be constant to maintain the same applied torque. Figure 6 shows an example of an MR-compatible ergometer using hanging weights [29].

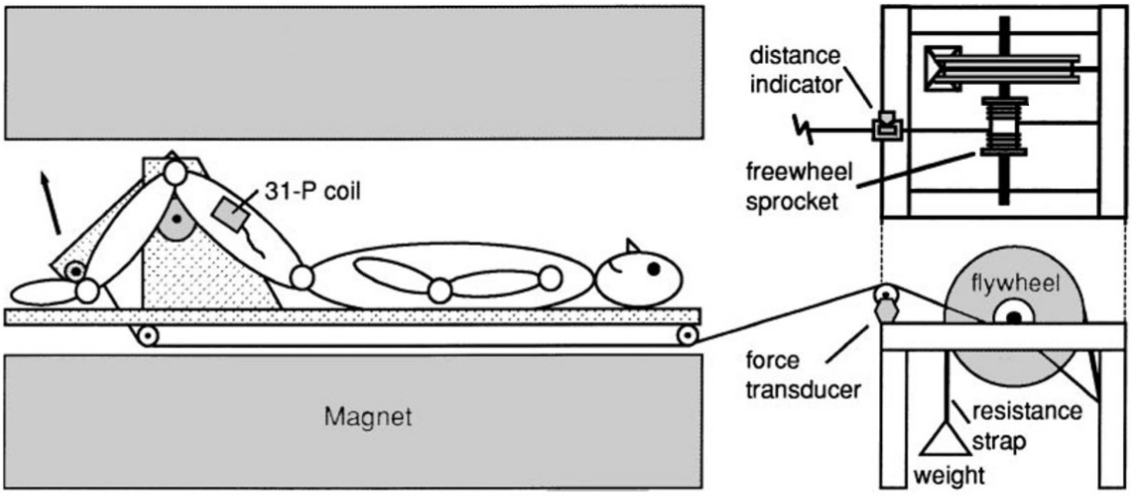

Figure 6: Hanging Weight MR-Compatible Ergometer

2.3.2 Active Designs

The previous passive designs were not capable of adjusting the load applied or the speed on the go to match a reference. As a result, none of them have the ability to subject their users to real isotonic or isokinetic contractions without unrealistically restricting their speed and acceleration. For those forms of contractions to be achievable inside the scanner, MR-compatible ergometers that control the applied load in real time are necessary.

One such design shown in Figure 7 makes use of an ordinary cycle ergometer placed in an adjacent room; the ergometer is connected to a passive cycling platform inside the MRI room using a system of rods and Cardan joints [23].

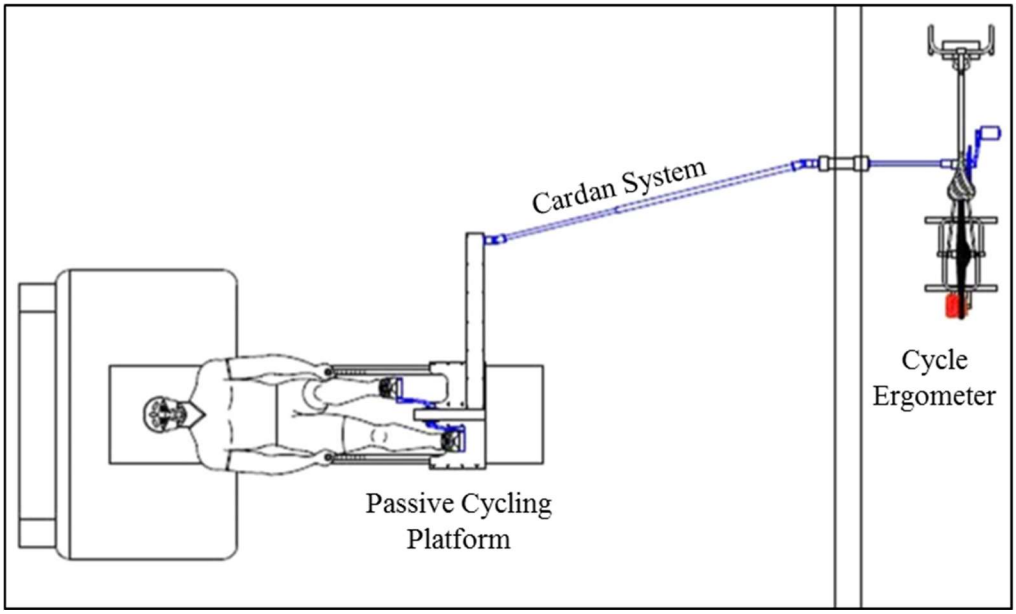

Figure 7: Cardan System MR-Compatible Ergometer

The design of this ergometer does not take the energy lost due to friction and the mass moment of inertia of the rods and Cardan joints in the mechanism into account. As a result, the energy and applied load measurements may not be accurate if those effects were significant.

A design that mitigates those potential issues transmits the power through a mechanical linkage. The design developed by Ryschon et el. [24] is shown in Figure 8. The resistive load is generated by a servo motor and measurements of the force applied are taken close to the pedal.

However, those measurements are not used for feedback, and the system is only designed for isokinetic contractions. The load data are used for logging and to calculate the work done.

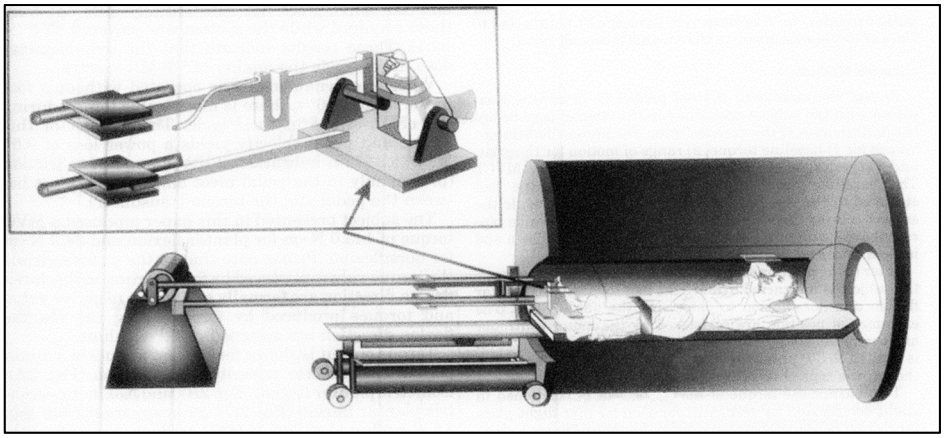

Figure 8: Mechanical Linkage Servo Driven MR-Compatible Ergometer

Having the source of the load closer to the user allows for more robust control and more accurate load application which is not possible in most cases that require direct control. However, a study done by Silmara et el. [32] managed to do that by using a friction based resistive load source. Figure 9 shows the design of this ergometer. The ergometer incorporates an aluminum flywheel which is designed to be rotated by the user while a brake is applied. The resistance of the brake is set by an operator in the control room, while both load and speed data are logged and used to calculate the power. The design could not be used for isokinetic contractions. The extensive use of powered elements fast moving conductive materials like aluminum means that a similar design could not be used inside the magnet for the study of the muscle it targets.

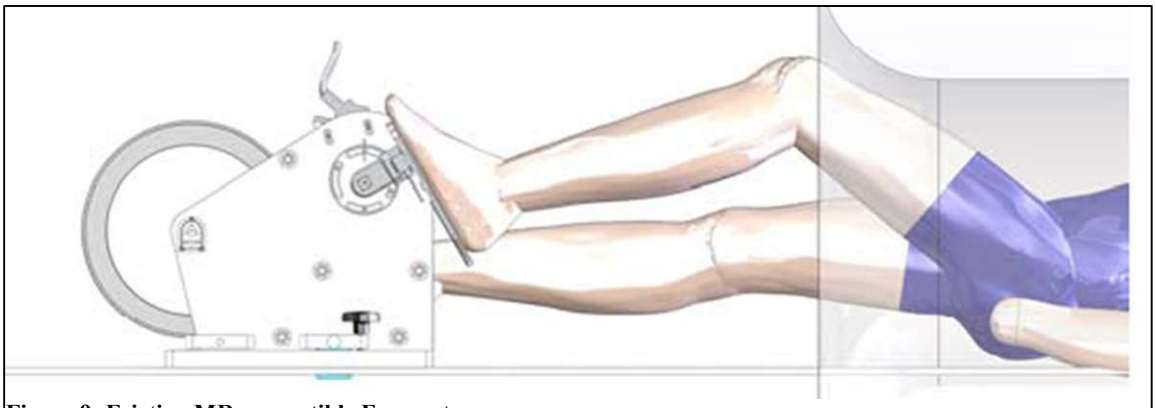

Figure 9: Friction MR-compatible Ergometer

In summary, most MR-compatible ergometers can apply loads for isometric and isotonic contractions. In many of those designs, the assumptions made meant that the contraction was not truly isotonic. One ergometer applied its load to stimulate an isokinetic contraction, but none were versatile enough to work with the three forms of contractions accurately. The fact that some of those ergometers focus on studying the heart or the brain means that some of their designs could not be used to study the active muscles inside the bore.

Unlike previously developed MR-compatible ergometers, the design presented in this work meets all of the following capabilities:

- Ability to stimulate accurately controlled isotonic, isokinetic, and isometric contractions.
- Ability to control the relation between the velocity and the load applied to maintain a constant power output through the contraction.
- Target the lower limb at high workloads while having the active muscles in the isocenter.
- Ability to directly measure and log the applied load, velocity and position in real time.
- Safe to use, and works well for a wide user base with different limb lengths.
- Easily operated using a simple user interface.
- Ability to provide real-time performance feedback to the person doing the exercise.

CHAPTER 3

SYSTEM DESIGN

3.1 Identifying the Required Design Specifications

The MRI machine used for this work is a three Tesla (3T) Siemens Skyra scanner with a 70-cm diameter bore. The device to be designed needs to target the lower limbs of its users by applying a load as a torque acting against knee extension. Additionally, the design should be reconfigurable into a device that can apply the load as a force acting against full leg extension. The area to be scanned using spectroscopy and imaging is the one containing the active muscles during the contraction, the quadriceps femoris.

The device should be capable of stimulating isometric, isotonic, isokinetic and constant power contractions about the knee joint while measuring load, velocity, and position. The resistive load applied has to be close to what a human can apply working in similar conditions. To specify that the limits for torque and speed are within the same 35 degree range of motion, data from three healthy male adults were collected using a Biodex dynamometer. The maximum torque recorded was 450 Nm in isometric mode. In the isokinetic test shown in Figure 10, a 500 degree per second limit on speed was used, and it gave a maximum speed of about 305 degrees per second or 5.3 radians per second. The test also shows the torque-speed characteristics of a user, which must be matched by the MR-compatible system developed.

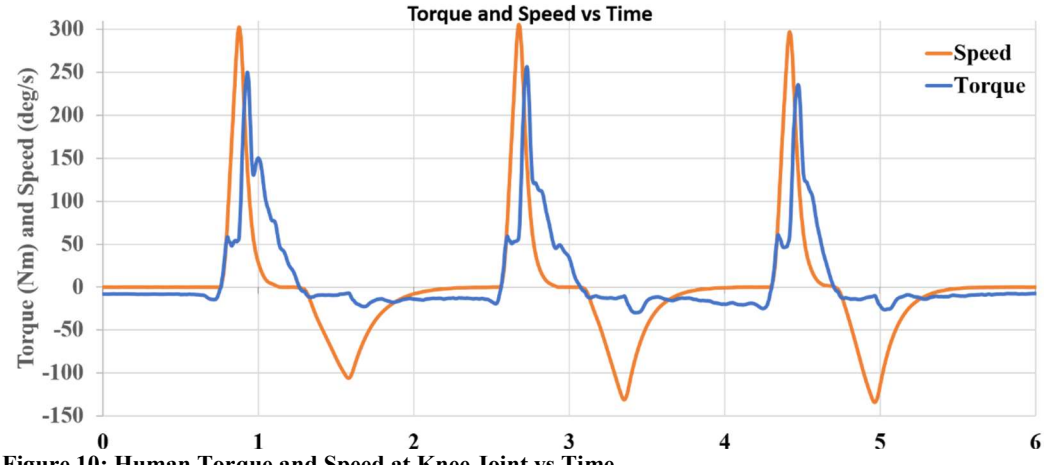

Figure 10: Human Torque and Speed at Knee Joint vs Time

There are also MR compatibility requirements on material selection and the restrictions on powered components. The design requirements categorized into three areas that are physical, performance, and MR compatibility requirements that are summarized in Table 2.

Requirement Area	Description
Physical Requirements	The part providing the resistive load has to fit inside a 70 cm diameter bore.
	The device should be adjustable to function safely and comfortably for its intended user base; In height, that is 95 percentile male to 5 percentile female (153 - 187 cm).
	The location of the device should ensure that the area to be scanned is close to the scanner's isocenter for all of its intended users. For a Siemens 3T Skyra, the recommended distance from the isocenter is lower than 10 cm.
	The required range of motion for knee extension is 35 degrees.
Performance Requirements	The ergometer should be capable of providing controlled resistive loads close to those produced by a human during the contraction. That is 450 Nm of torque and 5.3 radians per second for speed.
	The actuator applying the resistive load must match the speed-torque characteristics of the user, not just their individual peak values.
	The velocity, position, and force or torque applied must be recorded in real time at a sampling rate of 500Hz.
	The ergometer must be structurally strong enough to handle the predicted loading conditions (The loading conditions are dependent on the knee torque produced by a human, which is 450Nm).
MR-Compatibility Requirements	No magnetic or ferromagnetic materials can be used for parts in the bore.
	Materials with a magnetic susceptibly outside the range ($10^{-4} < \chi < -10^{-4}$) could not be used inside the bore.
	No large conductive loops near the targeted area to be scanned, or the body of the user.
	The length of conductive parts needs to be compared to the half-wavelength of the RF frequency inside it. The RF wavelength is dependent on the material and the nominal frequency, which is 128Mhz for a 3T Siemens Skyra MRI machine.
	Powered components should either be shielded and placed away from the area to be scanned.

Table 2: Design Requirements

3.2 Mechanical Design

The approach used to design for MR compatibility of the ergometer in this work is to avoid the use of powered elements near the scanner. Instead, all of the electrical aspects of both sensing and actuation take place away from the MRI machine, inside an adjacent room. Splitting the design into an active and passive component as shown in Figure 11 removes the limitation imposed by the magnetic fields on actuator and sensor selection. The passive component is actuated by the active one using a cable that passes through a waveguide and connects the two.

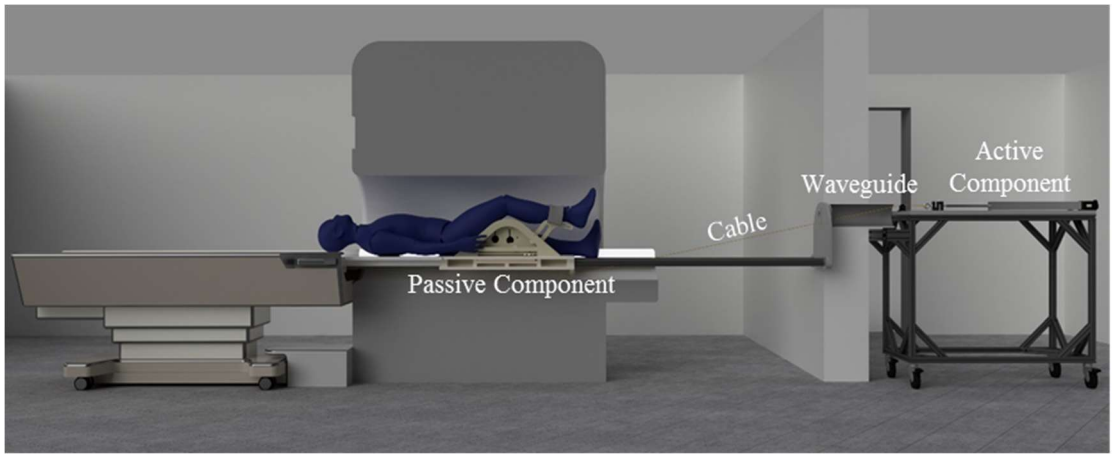

Figure 11: Ergometer Design Overview

The passive component was designed to fit inside a 70 cm bore three Tesla Siemens Skyra MRI machine while also being height adjustable to work with users of different limb lengths. The passive component has an isosceles triangular shape with 40-degree angles on each side setting the minimum starting knee angle for a user at 100 degrees.

With the ergometer setup to apply the load as a torque as shown in Figure 12, a curved beam is guided through a circumferential path using four wheels, two of which are mounted on cantilever beams. Those two cantilevers are pre-stressed to produce a force of 200 N perpendicular to the curved beam's surface to restrain its motion along the circumferential path. A pulley redirects the tensioned cable to meet the curved beam at a tangential point; this converts the applied tensile force in the cable to torque throughout the range of motion, which is 35 degrees.

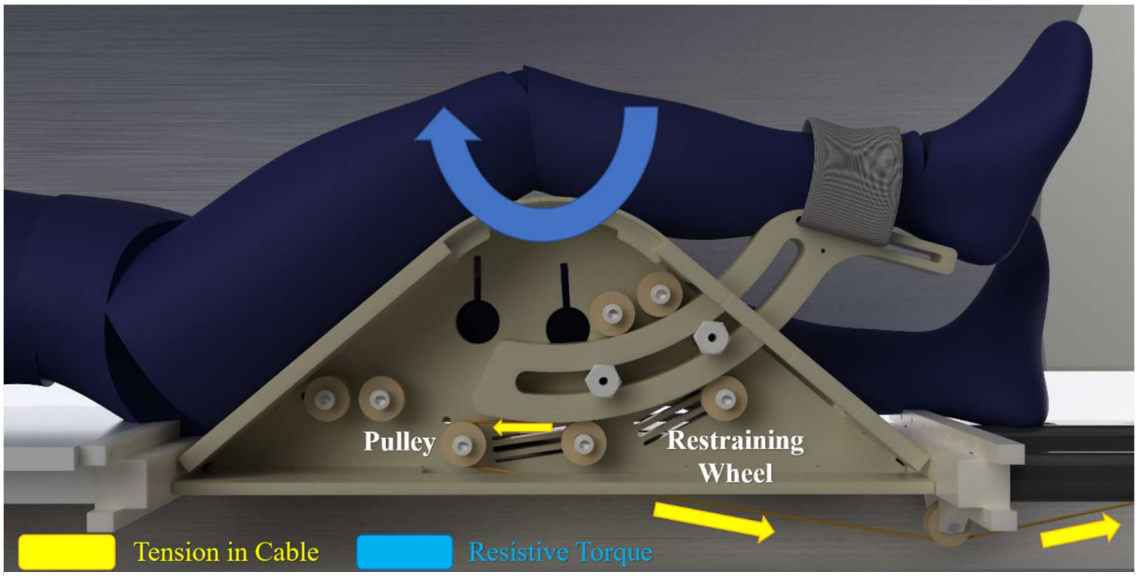

Figure 12: Ergometer Applying Resistive Torsional Load

Using a curved beam that moves along a circumferential path is advantageous to a piece rotating around a single hinge. If a single hinge was used, the knee joint could not be located at the center of rotation. As shown in Figure 13, this is necessary since the torque applied around the hinge will translate to a non-matching torque. In the figure, the radius R_1 is smaller than R_2. When a torque is applied by the device, a force will be produced on the strap, which will translate into a torque value that is scaled by a factor of R_2 over R_1 on the knee joint. Further, at different angles, the force produced will not necessarily be perpendicular to R_2, resulting in a force produced at the knee joint along with the torque. Therefore, a design with a single hinge is not desired.

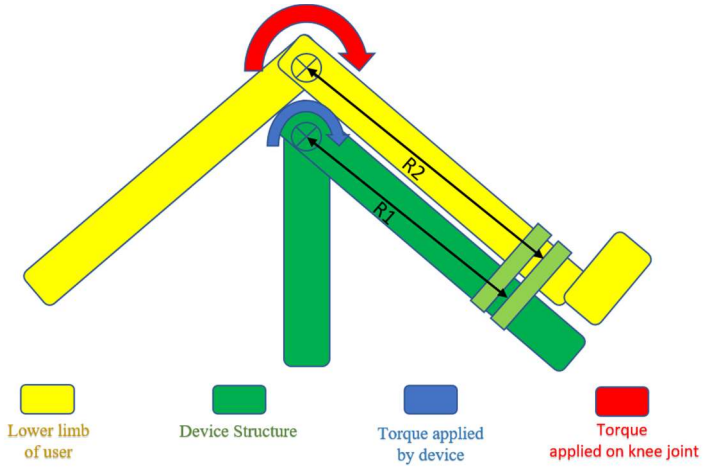

Figure 13:Translation of Torque for None Matching Axis of Rotation

Another approach to avoid those problems would be to use two hinges in parallel with the knee joint. However, this will add more weight to the moving part, increasing its moment of inertia and the minimum applied torque value. It also makes the design less flexible, making the switch to a linear mode significantly harder. Using a hubless design, the weight of the moving curved part was about 1.73 Kg, with the center of mass 292 mm away from the axes of rotation (Moment of inertia is 0.15 $Kg.m^2$). The angle relative to gravity ranges from 12 to 47 degrees, resulting in a maximum torque difference of 2.3 Nm due to gravity.

The frame of the ergometer, the moving curved piece, and its mounting platform were made out of Nylon 6/6 sheets, which were computer numerical Control routed or waterjet cut, then assembled together using nylon bolts. Two 3D printed Acrylonitrile Butadiene Styrene (ABS) plastic parts with an aluminum core inside act as mechanical end stops to restrain the beam from going over its intended range of motion. They are also used to reduce friction and to keep the curved beam from wobbling. End stops can be removed so that the curved beam can be replaced with the straight one or for the cable to be easily replaced. Polyether ether ketone (PEEK) wheels and pulleys riding on ceramic bearings (Boka, LC-6900) were used to guide a moving part through a circumferential or linear track based on the mode. The only metallic parts used were the shafts for the wheels and pulleys and the core for the mechanical end stops which were made out of 7075 aluminum.

The aluminum pieces used are surrounded by PEEK, Nylon 6/6 or ABS plastic. To calculate the lengths to be avoided, the dielectric constant is set to 3.2 for PEEK, 5.7 for Nylon 6/6, and 3.3 for ABS plastic, the nominal frequency is set to 128 MHz and Eqn. 1 was used to calculate the maximum material lengths. For aluminum parts surrounded by PEEK, the half wavelength is 65.5 cm, 49.1 cm for parts surrounded by Nylon, and 65.3 cm for parts surrounded by ABS plastic. The longest aluminum piece used in the design is 22 cm. Thus, the RF field

should not cause a problem. The aluminum parts do not move when the device is operational either. Therefore, the static magnetic field will not produce induced currents inside them.

The ergometer can be fitted in place using a platform that slides into the rails of the scanner. That platform along with two keys that lock the ergometer to it, restrain the ergometer from moving vertically or to the sides. The keys also act as a mechanism used to adjust the height of the ergometer to fit people with different femur lengths. The ergometer was designed to work with users of heights ranging from the tallest 95th percentile male to the shortest 5th percentile females. Height data from the Center for Disease Control [33] were used to get the height range, which came out to be 153 - 187 cm. To calculate the femur lengths using the height of the user, an equation developed in [34] was used:

$$Stature(cm) = \begin{cases} 2.47 * Femur\ Maximum\ Length(cm) + 54.7, & Female \\ 2.38 * Femur\ Maximum\ Length(cm) + 61.41, & Male \end{cases}$$

The equation, along with the height data gave a range of the femur length going from 39.7 to 53.4 cm. Since the thigh rests on the ergometer at an angle of 40 degrees, the range of height adjustment for the ergometer becomes: (53.4 -39.7) sin(40) = 8.8 cm.

One millimeter is added to the lower and upper limits making the range in height adjustment 9 cm, and that range was divided into five settings 1.8 cm apart, each of those is to be used with a corresponding user thigh length bracket, those brackets are:

$$Height\ Setting\ = \begin{cases} 1, & Thigh\ Length(cm) \geq 50.8 \\ 2, & 50.8 > Thigh\ Length(cm) \geq 48.1 \\ 3, & 48.1 > Thigh\ Length(cm) \geq 45.3 \\ 4, & 45.3 > Thigh\ Length(cm) \geq 42.6 \\ 5, & 42.6 > Thigh\ Length(cm) \end{cases}$$

The keys that lock the ergometer to the sliding platform go into one of the five slots, each setting the height of the ergometer to accommodate a different femur length bracket. Figure 14 shows the process of installing the sliding platform with the ergometer into the scanner:

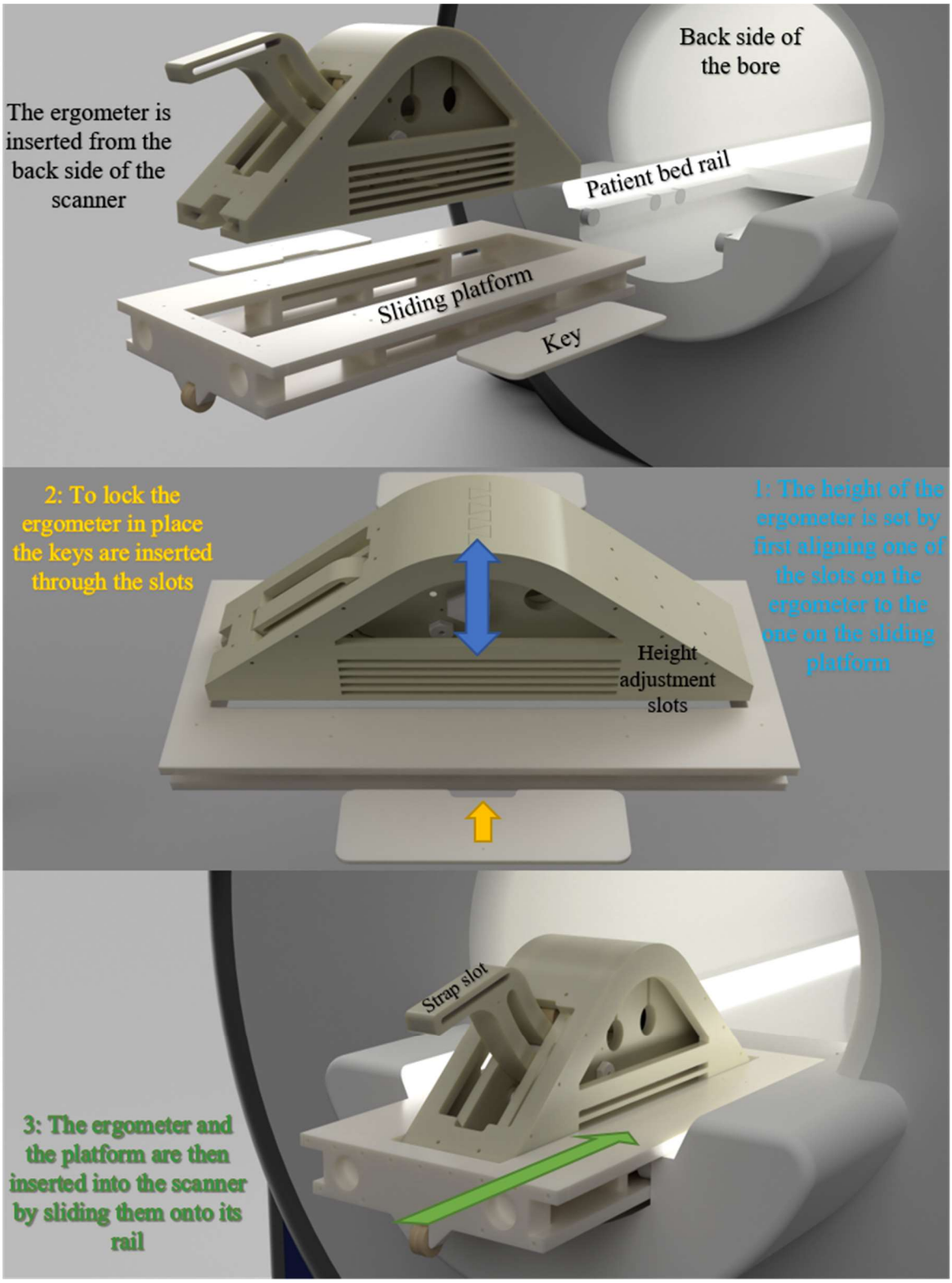

Figure 14: Process of Installing Ergometer

The leg of the user is attached to the leg rest piece on the end of the curved beam using Velcro straps that loop through a slot (Figure 15). The distance between the knee joint and the Velcro attachment point can be changed to accommodate users of different tibia lengths. The adjustment is done by sliding the Velcro along a slot below the foot rest. Equations developed by Izzet Duyar et al. [35] were used to calculate the distance range to be covered by the slot.

$$Stature(mm) = \begin{cases} 951.94 + 1.890 * Tibia\ Length(mm), & Stature \leq 1{,}652 \\ 944.82 + 2.057 * Tibia\ Length(mm), & 1652 > Stature > 1841 \\ 1224.15 + 1.530 * Tibia\ Length(mm), & Stature \geq 1841 \end{cases}$$

The resulting range is from 295 to 431 mm. The slot was designed to accommodate a range from 290 to 435 mm, 55 mm was added for Velcro straps with a width of two inches to be used. This makes the total width of the slot 200 mm.

To prevent the ergometer from moving horizontally along the bore of the scanner, a part that supports it against the wall of the room was built. The structure opposes the cable forces as shown in Figure 15. Two of 2-inch diameter polyvinyl chloride (PVC) rods connect the sliding part to a wall support plate which spreads the stress over a large area while also acting as a cap for the waveguide. The length of the two PVC rods is 1.71m, it is set to place the quadriceps muscles of the user at the isocenter of the scanner.

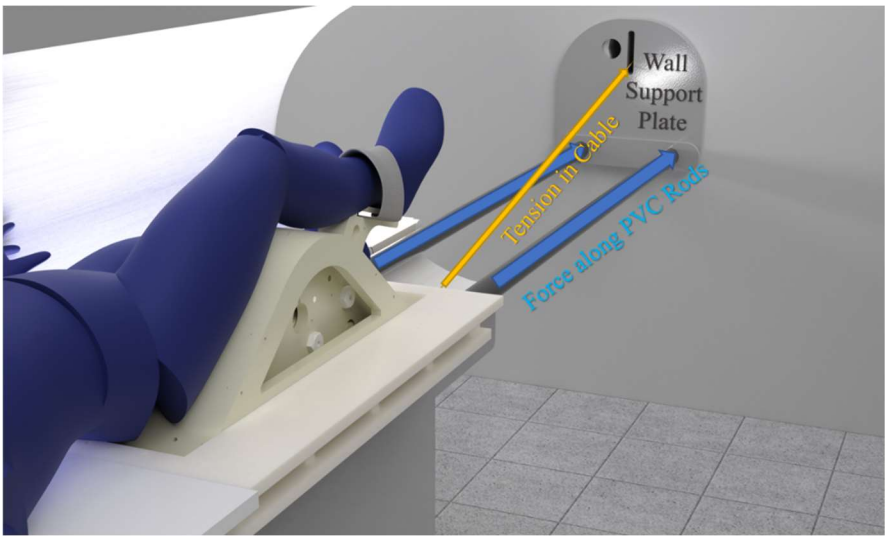

Figure 15: Wall Support Structure

Due to the limited space left on the bed after the coil connectors are places, a plate is used as an extension to the platform, supporting the back of the user and preventing the ergometer from sliding further into the scanner. The ergometer is positioned in a way that keeps the coil placed on the thigh of the user close to the isocenter of the MRI machine.

In the second mode of operation, the curved beam is replaced with a straight one as shown in Figure 16. The straight beam is guided by three wheels, one of which is mounted on a cantilever beam spring. Another pulley redirects the tensioned cable to move along the lower side of the beam and connect to its end. This tension is transmitted through the beam as a force acting against the leg during extension.

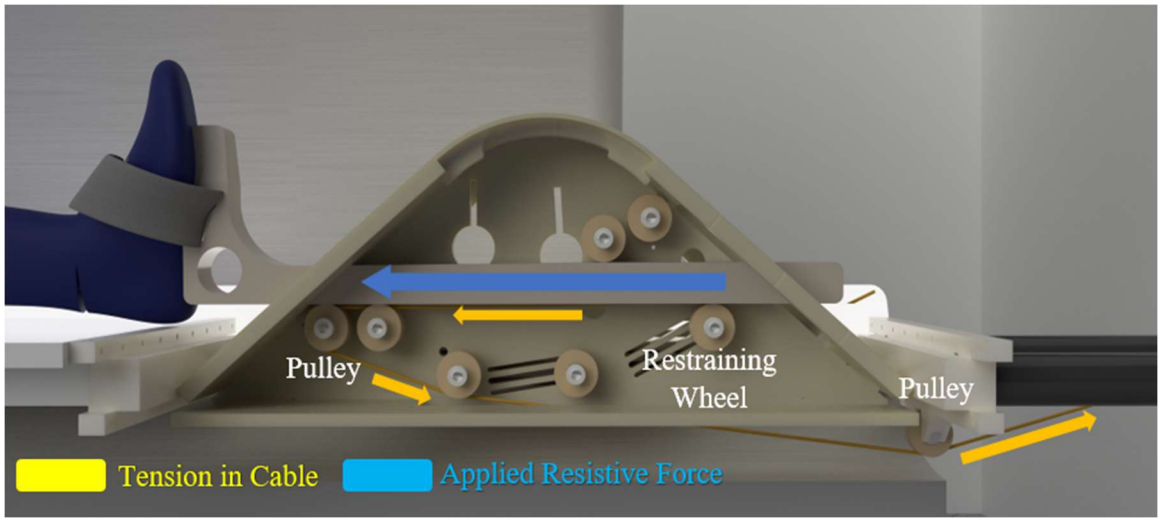

Figure 16: Ergometer in Linear Mode

A custom cart made out of extruded 8020 aluminum is used as a platform to hold an AC servo driven linear actuator as shown in Figure 17. It also holds the powered sensors, the weight lifting mechanism used for initial testing, and some other electronics. The cart is designed to carry a load of up to 300 kg vertically. It also has a portion that distributes the linear actuator's reactive force acting horizontally on the wall. The linear actuator is mounted on top of a 25.4 mm thick PVC sheet top which transfers the load over to the aluminum structure underneath it.

A load cell connects the rod end of the actuator to the cable, which is passed onto a pulley mounted close to the waveguide. The angle between that pulley and the ergometer allows the cable to pass through without touching the waveguide.

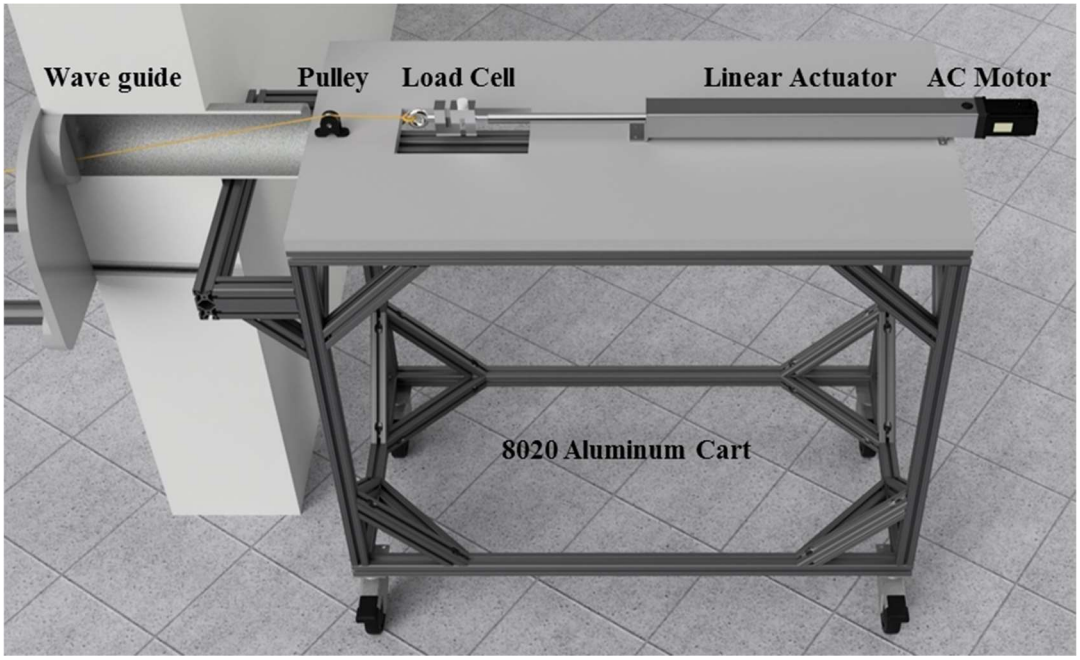

Figure 17: Linear Actuator Table

The cable used was a 3mm diameter sheathed Dyneema cable rated at 1000Kgf. Other cables were also tested each with shortcomings; a 1/8th inch diameter braided Kevlar cable was hard to terminate securely. A 1 mm diameter sheathed Spectra cable was slipping between the pulley and the moving part frequently, and a 3mm diameter braided spectra cable was more susceptible to wear and had less compliance than the Dyneema cable.

3.3 System Architecture

Locating all of the active components of the ergometer outside the scanner's room removed many of the powered component restrictions imposed by being near the field. The main design requirements left for most components of the system are related to the load to be applied and the quantities to be measured or controlled.

3.3.1 Actuator Selection

The motor and linear actuator were selected to provide torque/speed characteristics matching those of a human user operating with the same range of motion in the torque mode (35 degrees). In initial testing, using a Biodex dynamometer, the peak recorded values for torque and speed were 450 Nm and 5.3 rad/s. For a 35 cm radius, those numbers translate to 1286 N and 1.86 m/s linearly.

A back-drivable ball screw (Thomson, PC-40) with a 20 mm lead and an 40cm stroke was selected as the transmission of the linear actuator. It has a maximum dynamic load of 1500 N and a maximum speed of 1.67 m/s. A back-drivable transmission allows for resistive loading since the torque produced by the user will be back driving the linear actuator while the motor torque acts against it.

A Yaskawa SGMJV-06A AC servo motor will be used to drive the ball screw. The motor can provide a torque of up to 6.69 Nm and rotate at a maximum speed of 6000 RPM. The motor was matched with a Yaskawa 5R5A driver rated at 0.75 KW. Figure 18 shows the data of Figure 10 mapped onto a predicted required motor speed torque curve. A simulation built using the datasheet of the Thomson PC40 ball screw was used to do the mapping. The curve is overlaid on top of the motor's peak and continuous torque-speed characteristic curves.

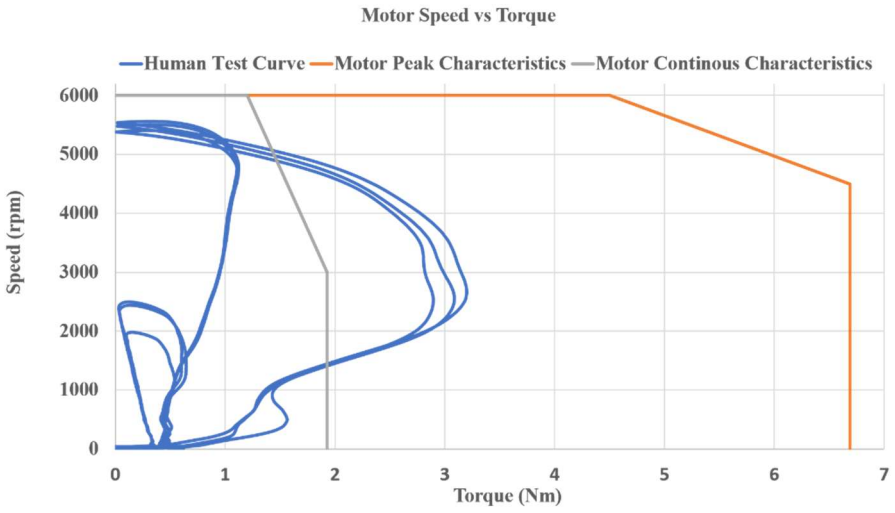

Figure 18: Human Torque Speed vs Motor Torque Speed Characteristics

When the torque of the motor is applied as a resistive load, the motor acts as a generator, and an integrated dynamic braking circuit is used to dissipate the energy. The motor and driver have a peak power of 3.15KW, and the max power in the mapped curve was 1.16KW. With both the motor and the linear actuator, the system should be capable of applying a torque of up to 420 Nm at speeds of up to 4.7 rad/s. In the linear mode, the maximum force that can be applied by the ergometer is 1200 N and the speed peaks at 1.667 m/s.

3.3.2 Sensing

For the ergometer to work properly, the load applied by the user, the speed at which the user is moving their leg, and its position will need to be measured. A single axis S-beam load cell (OMEGA, LCM115-500) is used to measure the load applied. It has a 500 kgf load capacity which is higher than the expected 122 kgf for the system. The load cell is placed between the actuator and the cable to measure its tension. The load cell signal is amplified to a range of 0 - 3.3V signal and then outputted to analog to digital converter on a microcontroller. A 20-Bit absolute encoder is used to measure the speed and the position of the user. The system is configured to translate the encoder signal to a 12,000 pulse/revolution quadrature encoder output. With a lead of 20 mm, this translates to a resolution of 8.33×10^{-4} mm linearly or 13.6×10^{-5} degree.

3.3.3 User Interface and Audiovisual Feedback

A MATLAB user interface was developed to enable easier control of the system, serial data logging, and to provide the participant with audiovisual feedback. The main screen of the user interface has four mode selection buttons (one for each contraction type), the serial port selection textbox, a start/stop button, and a button used to save data (Figure 19). The main screen also shows a real-time stream of either torque or position data normalized over a configurable maximum value. The stream can be configured to also show a target line indicating what is

required from the participant to achieve. The same screen is mirrored to a fiber optic monitor inside the magnet room for the participant to get feedback on his performance in real time.

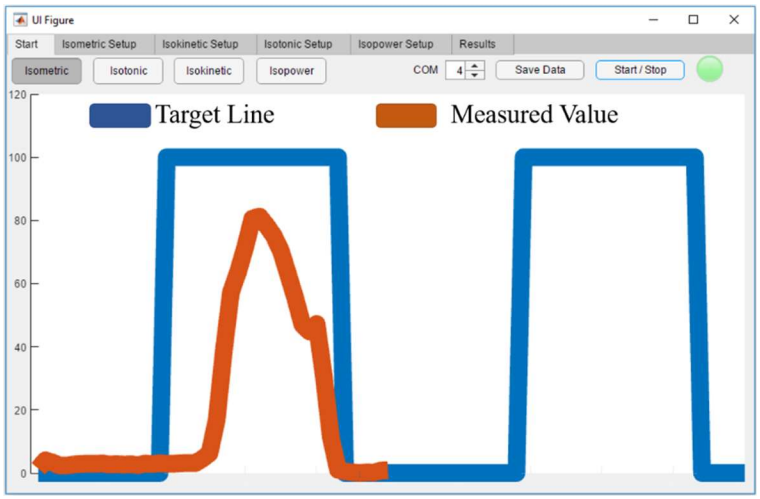

Figure 19: User Interface Main Screen

Each contraction type has a specific setup screen allowing the user to configure a test protocol (Figure 20). In each mode, the user can change the reference value (torque for isotonic, position for isometric, velocity for isokinetic, and power for the constant power mode). Other parameters that can be modified are the contraction duty cycle, the range of motion, the starting angle, the value to normalize by, the initial cable tension value, and the target line value, which is the value the participant is required to hit in each contraction.

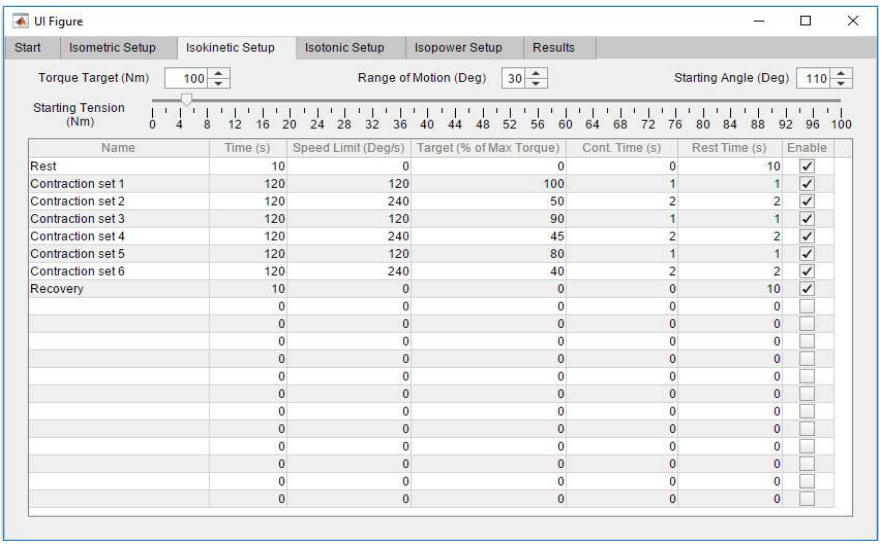

Figure 20: Ergometer Setup Screen

The program also sounds a signal at the start of each contraction that can be heard in the magnet room. The signal helps the participant sync the end of the contraction with the RF pulse of the scan sequence.

The data are automatically analyzed at the end of the test protocol, and a contraction by contraction data matrix is displayed in the results section, and saved if the save button is pressed. The results show the maximum torque, velocity, and power for each contraction with a corresponding position value along with the maximum position value and the energy excreted for each contraction.

3.3.4 System Architecture Overview

The system shown in Figure 21 consists of a computer with the user interface, which communicates serially with an Arduino Due microcontroller. The Arduino is connected to a load cell amplifier; it also receives the processed motor encoder signal coming from the driver. Analog speed and torque control signals are passed onto the motor driver (Yaskawa, SGDV 5R5A). Data acquisition and processing tasks are done on MATLAB.

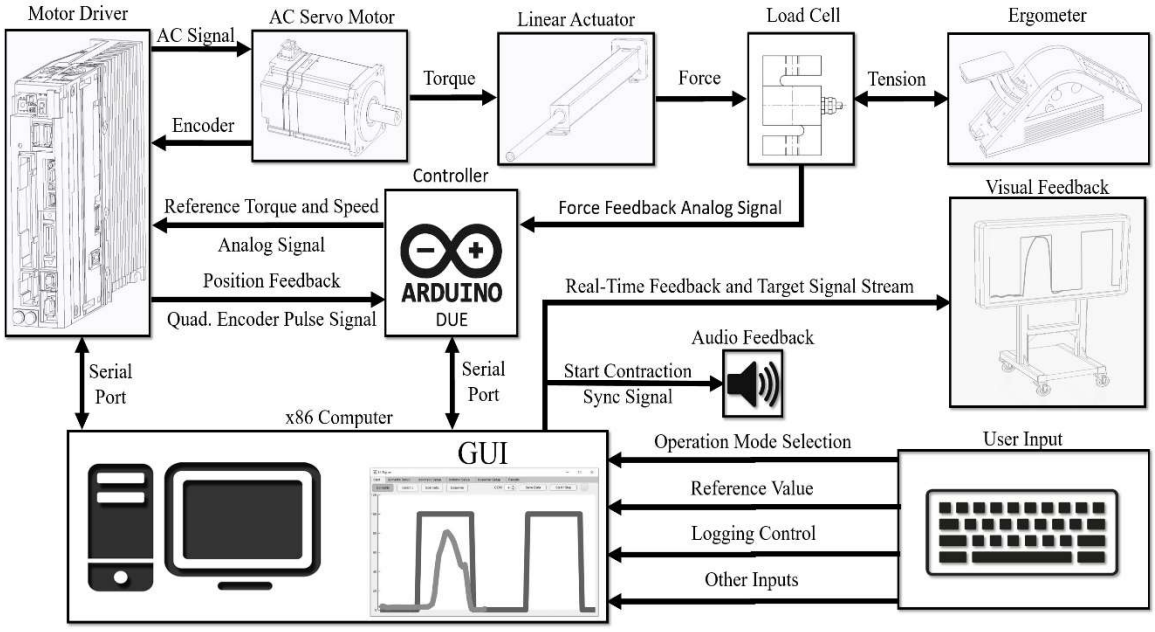

Figure 21: System Architecture Overview

CHAPTER 4

CONTROL

4.1 Signal Processing:

The microcontroller used is an Arduino Due with an 84Mhz Atmel SAM3X8E microprocessor. It has two integrated digital to analog converter (DAC) channels, 12 analog to digital converter (ADC) channels, and dedicated quadrature decoder hardware. The firmware is designed to handle all control tasks by itself after receiving an instruction from the computer. The instruction can specify the mode of operation along with reference values. Position, velocity, and torque are sampled at 4 kHz and are sent to the computer at a rate of 500 Hz.

The use of an AC servo driver with very high-speed switching elements introduces noise to the system. The switching noise is only a problem for the load cell signal after amplification in this case since it is the only analog signal going into the microcontroller. The noise profile of the amplified load cell signal was sampled at 1 kHz with all hardware filters removed. Figure 22 shows the noise signal with the motor activated.

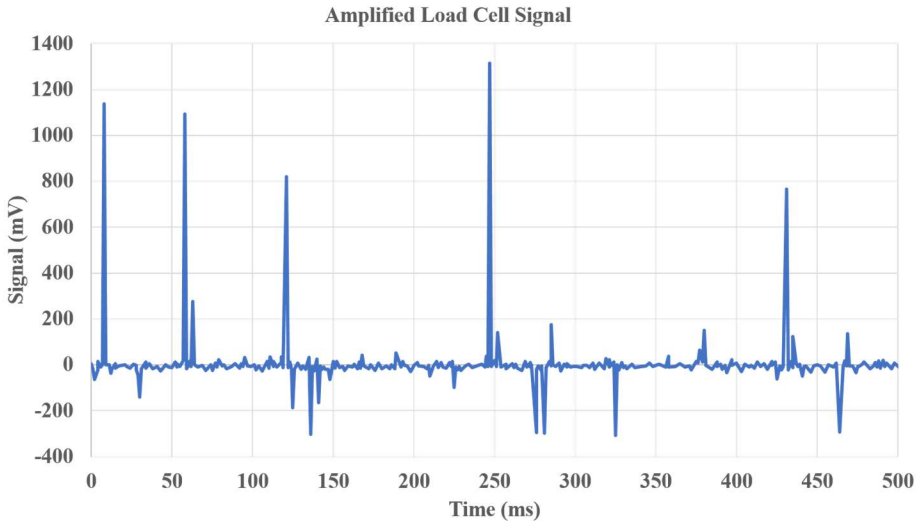

Figure 22: Switching Noise in Amplified Load Cell Signal

The graph shows that the noise comes in pulses that last for a very short period (one sample). Using a moving average or an exponential low pass filter would reduce the noise amplitude, but it would also distribute the error in the pulse samples to the rest of the signal.

Another approach would be to use multiple ADC channels at the same time [36]. Taking the average of all channels and applying a low pass filter, the noise amplitude would be reduced further. However, this will still add noise to the signal near pulse samples.

Selectively attenuating pulse samples before applying a filter is a better approach. To do that, a function that saturates change from one sample to the next is used. The saturation limit should be higher than the maximum rate of force production (RFD) of the targeted muscles [37, 38]. It should also be high enough for the derivative component of the PID controller to be effective. The limit used was 2.45 mV per sample at 4 kHz and is equivalent to an RFD of 2000 Nm/s. The peak RFD value in two studies [37, 38] were 1899 Nm/s, and 4.33 N of peak force per second, or 1818 Nm/s at a peak torque of 420 Nm, both RFD values are lower than 2000.

Four analog to digital channels are used to read the analog signal, the maximum and minimum samples are taken out to eliminate most spike samples. The two remaining samples are averaged and inputted into the rate saturation function. An exponential 200 Hz low pass filter is then used giving a relatively clean output with an error of ±0.36 Nm. Figure 23 compares the output of this method to a single channel and a four-channel 200 Hz low pass filter.

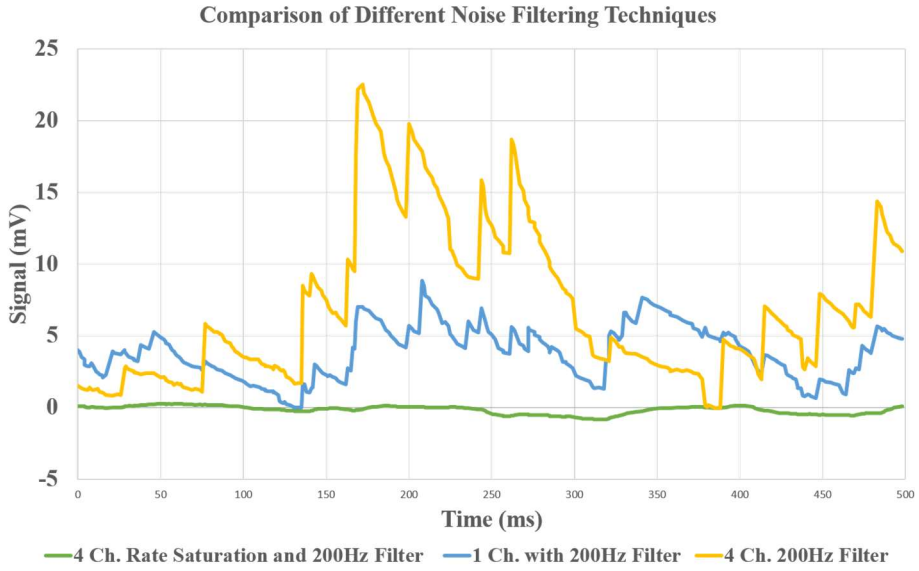

Figure 23: Noise in Load Cell Signal Filtered Using Different Methods

The encoder signal is processed using the built-in microcontroller hardware. At 12,000 pulses per revolution, the position reading resolution is 13.6×10^{-5} degrees. However, due to stretch in the cable, and elastic deformation of the system, the position value needs to be corrected. Torque data collected from the load cell are used to account for stretch, making the position sensor more accurate. The stiffness of the system was calculated with the ergometer locked at zero degrees, and the actuator was used to produce a torque of 100 Nm gradually from 20 Nm. The test was repeated four times while the angle and torque values were sampled at 500Hz. Figure 24 shows the torque versus angle for all four tests.

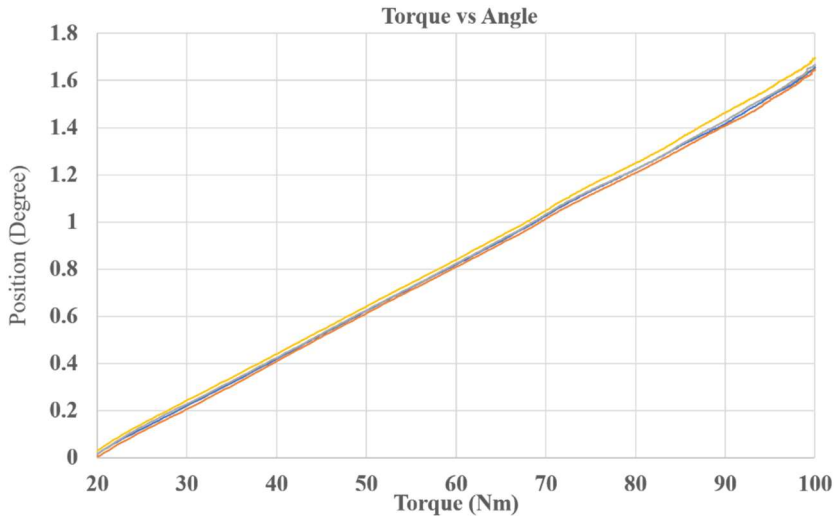

Figure 24: System Stiffness Evaluation

Using linear curve fitting, the value for stiffness was 2781± 26 Nm/rad results in a correction factor of 0.0206 degrees/Nm. This value will be multiplied by the torque reading and added to the position by the microcontroller. The velocity is calculated by differentiating the position signal. Both position and velocity signals pass through a digital 200 Hz low pass filter before being logged. This is done to smooth both signals and to synchronize them with the torque data without having to create an array in the microcontroller.

Also, the torque signal is corrected to account for gravity and the moment of inertia of the moving parts of the device. The effect of gravity on the torque value is ±1.15 Nm through the range of motion. Torque due to the moment of inertia is significant only at the start of isokinetic

and low torque isotonic contractions, velocity is either constant or changes very slowly in all other cases. Figure 25 shows an example of an isokinetic contraction signal before and after torque correction.

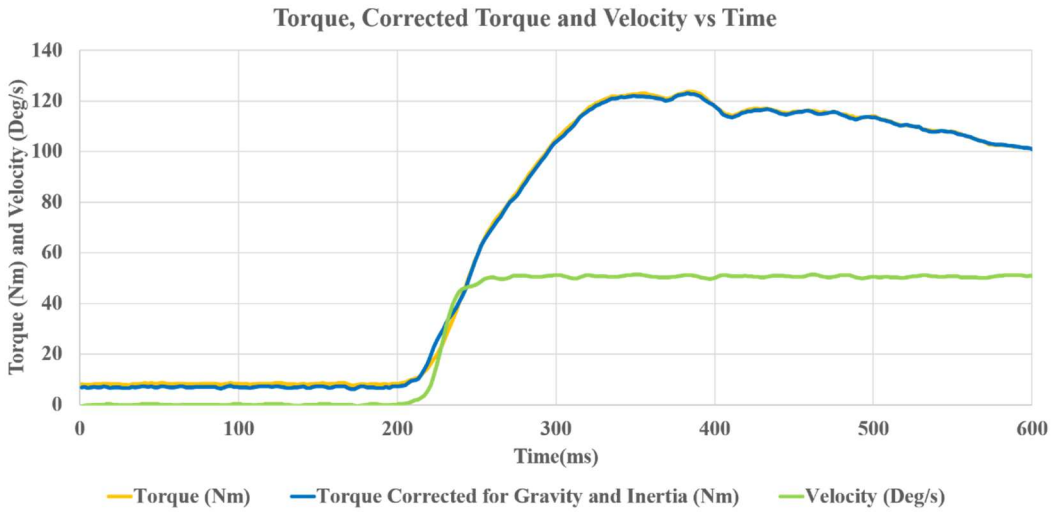

Figure 25: Isokinetic Contraction with Corrected Torque Signal

4.2 Position, Torque, and Velocity controllers.

Two digital to analog channels are used to send a control signal to the motor driver. The two signals go through a differential amplifier producing a ±10 V analog output. The voltage value is read by the driver and is used to change the characteristics of the AC signal going into the motor. The driver can be configured to map the analog reading to either speed or torque, for this application, and in all control modes, the driver is setup to map the voltage to a torque value.

To control position, the encoder reading combined with the load cell reading for stretch correction are combined to get the corrected position reading. The corrected position is used for feedback, and the DAC channels are the controller output. The reference is set using a serial command ("PRX", where R is the position reference in degrees). Figure 26 shows the block diagram of the position controller.

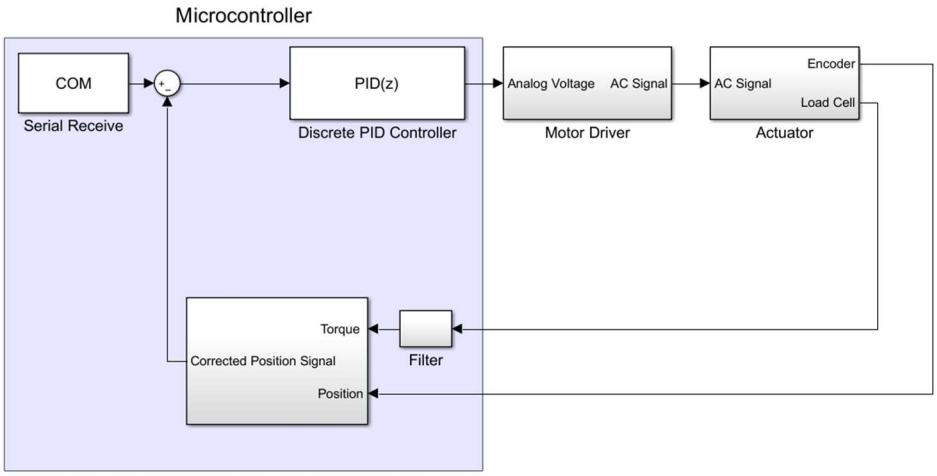

Figure 26: Position PID Controller Block Diagram

To control velocity. The position signal is derived and used for feedback, and the DAC channels are used for output. The reference is again set using a serial command ("VRX", where R is the velocity reference in degree/s). Figure 27 shows the block diagram of the velocity controller.

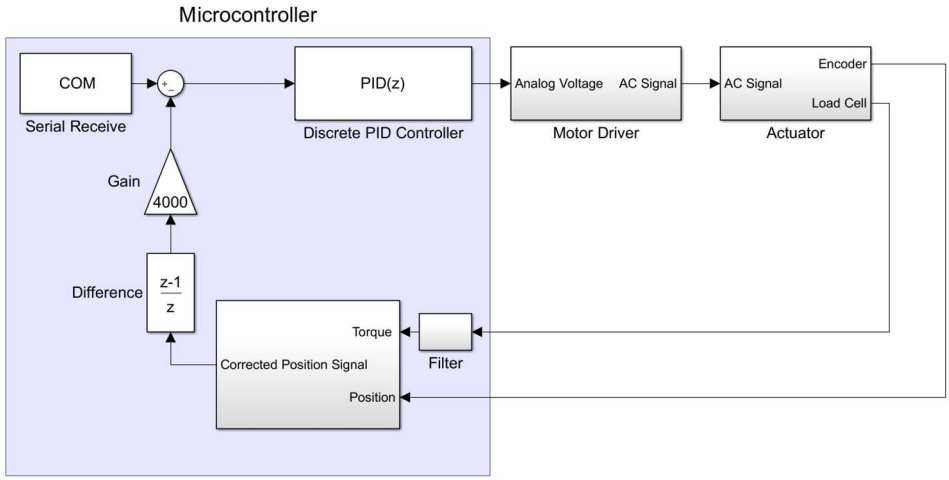

Figure 27: Velocity PID Controller Block Diagram

Due to the nonlinearity of the system, its behavior changed depending on the torque produced on the ergometer. This change in system behavior made tuning the torque controller with a single set of gains across a wide range of torque values difficult, and it required that multiple PID controller gains be used for different reference brackets. Four controller gain brackets were defined: Less than 6 Nm, 6 to 40 Nm, 40 to 75Nm, and higher than 75 Nm. The

controller gains were tuned for robustness at lower reference values and were lowered at higher values to keep the system stable. Figure 28 shows the torque controller block diagram. The torque controller reference is set using a serial command “TRX” where R is the reference value in Nm.

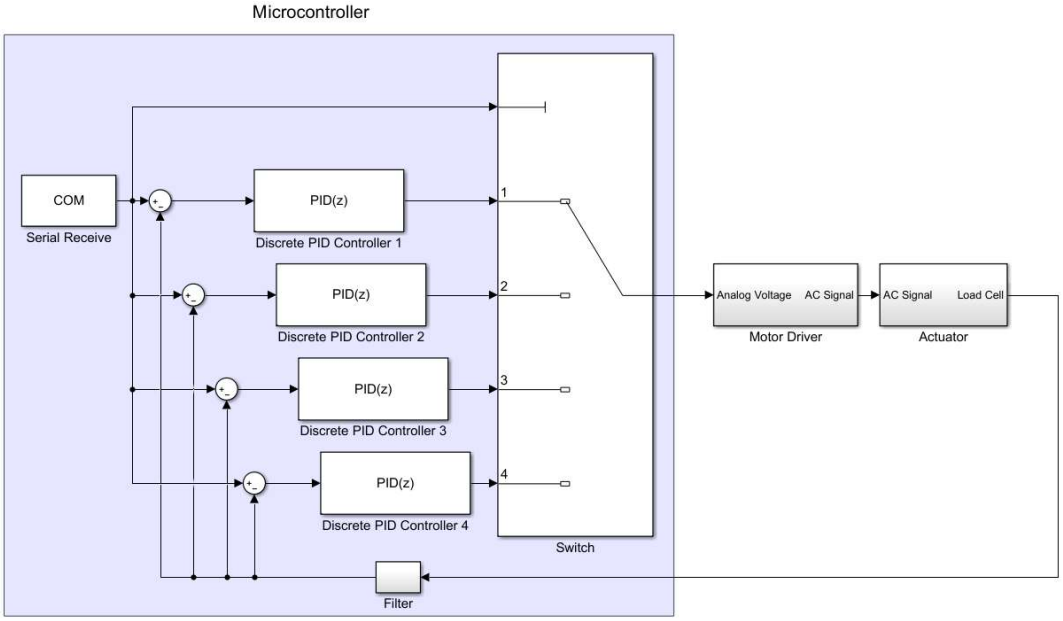

Figure 28: Torque PID Controller Block Diagram

4.3 Isometric Mode

To start the isometric mode, a serial command “M” is sent. The controller starts by applying a small amount of tension to the cable and moving to the zero position; this is done using the torque controller. After 500 ms, the controller checks that the tension value exceeds the amount set and starts the position controller. The user will then apply torque to the ergometer, which gets transferred to the actuator via the tensioned cable. The position controller applies a load to resist motion and stay at the zero position. The torque value is sampled at 4 kHz filtered and sent to the computer serially at 500 Hz.

4.4 Isotonic Mode

The isotonic mode starts with a serial command “IRX” where R is the torque reference in the extension portion of the contraction. Another command “LRX” sets the range of motion (‘R’ is the range in degree). Figure 29 shows the finite state machine diagram of isotonic mode. In this mode, the controller starts by applying an initial tension value for 500 ms. Then, after checking

that the tension value has exceeded the amount set, the controller then zeroes out the position reading and changes the torque to the extension torque reference value. The user will then start moving their leg against the resistive load of the ergometer. Once the user reaches the maximum range of motion specified, the controller switches to position control mode preventing the user from moving further. When the user starts moving their leg down, the torque value drops below the flexion torque reference (default is 10 Nm). The controller switches back to torque control mode this time with the reference set to the flexion torque value. When the leg position is close to zero and with the velocity near zero as well, the torque reference switches back to the extension value. The controller can also switch from the flexion torque state to position control if the user exceeded the range of motion in that state.

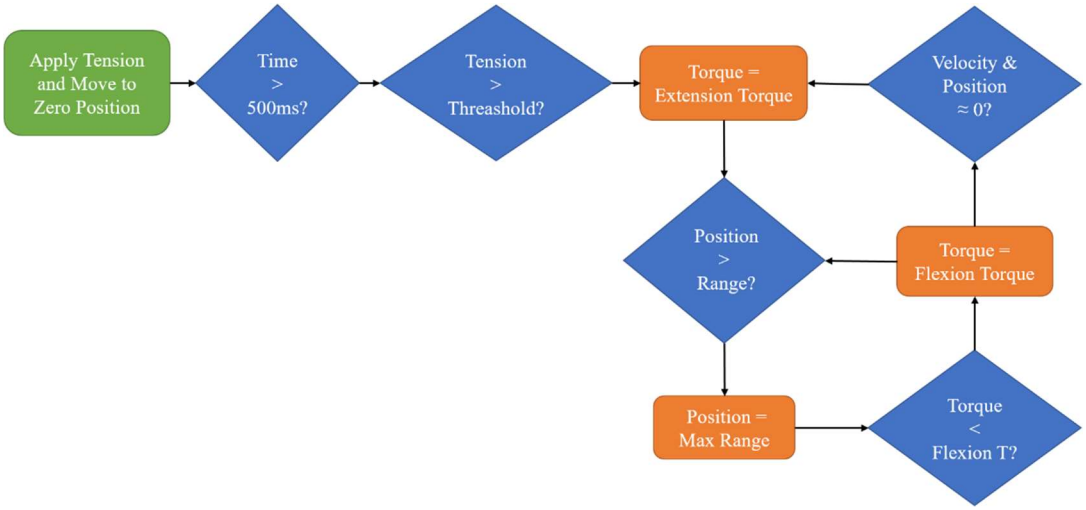

Figure 29: Isotonic Controller Finite State Machine Diagram

To ensure stability, changing the torque reference is done gradually using a 4 Hz digital exponential filter applied to the step input. If the torque reference were to change from 10 Nm to 100 Nm, for instance, it would do so gradually over about 250 ms.

4.5 Isokinetic Mode

To start isokinetic mode, a serial command “KRX” is used where R is the velocity limit reference in degree/s. The range of motion is set using the same “LRX” command. The finite state machine diagram of the Isokinetic Mode controller is shown in Figure 30. Once the serial command is received, the controller applies the initial tension value moving to the zero position and resetting the encoder reading to zero. After that, a low extension torque value is applied (default is 5 Nm). The user then extends their leg and either reaches the isokinetic velocity limit specified or reaches the range limit before that. If the range limit is reached first, the controller switches to position control, limiting motion over the range. From that point, the controller behaves like an isotonic controller until it gets back to the extension state. If the velocity limit is reached in extension mode, the velocity controller maintains the velocity at the reference value. The velocity is maintained up to the range limit, or if the user slows down before reaching the limit, the controller switches to the flexion state. The controller can also switch from the flexion state to position control if the user exceeded the range of motion, or to velocity control if the velocity exceeded the limit set in that state.

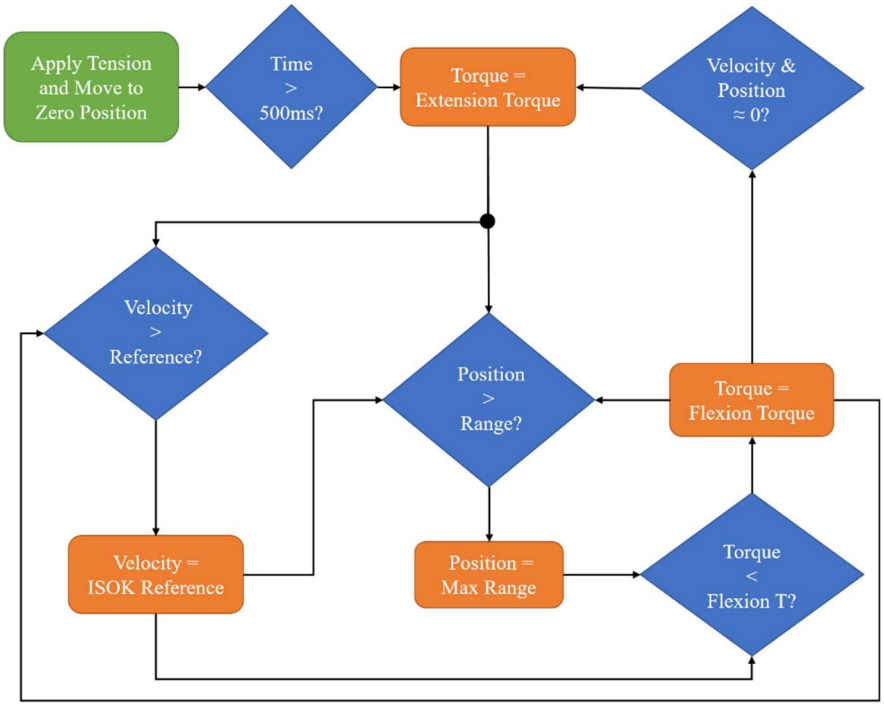

Figure 30: Isokinetic Controller Finite State Machine Diagram

4.6 Constant Power Mode

The constant power mode is initiated with a serial command "WRX" where R is the power reference in Watts. The range is set using the "LRX" command. Figure 31 shows the finite state machine diagram of the constant power controller. The controller initiates by applying tension for 500 ms to move to the zero position. After that, the position controller locks the ergometer until an isometric torque satisfying the equation ($T = \frac{Power\ Reference}{Initial\ Velocity}$) is measured. The initial velocity value is determined based on the power reference. Starting at 2 rad/s for a reference value less than 100 W and increasing linearly with the power reference value at a rate of 2.5×10^{-3} rad/s.W. When the torque limit is reached, the velocity controller starts, changing its reference based on the torque to maintain a constant power draw. This is done until the position is higher than the range limit, after which point, the controller switches to position control. When the torque drops below the flexion torque limit (default is 5 Nm), the controller switches to the flexion state. Then, once the velocity and position readings are close to zero, the position controller kicks in locking the ergometer at the zero position again. The velocity reference value is restricted to be higher than zero radian and less than 4.7 rad in this mode.

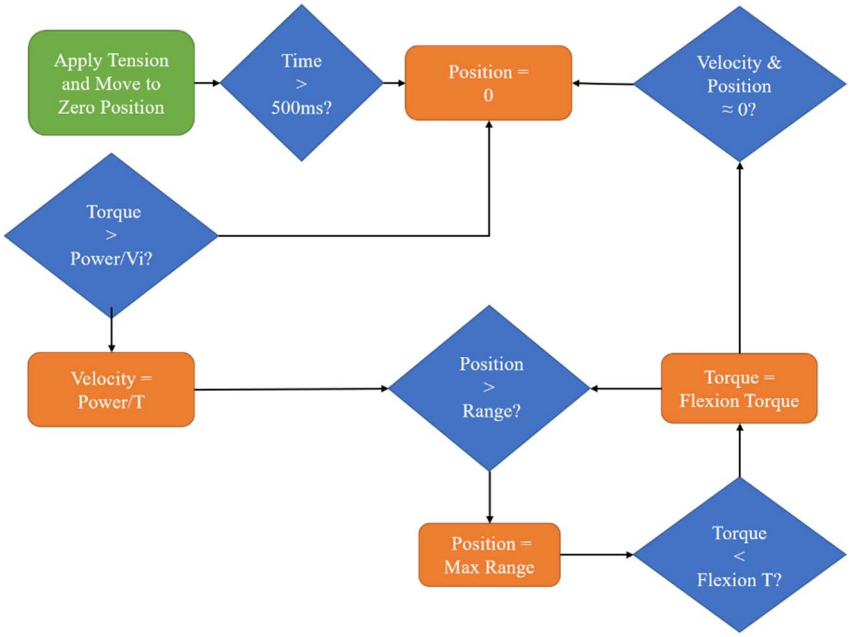

Figure 31: Constant Power Controller Finite State Machine Diagram

CHAPTER 5

RESULTS

5.1 Position Controller Performance Evaluation

The position controller was tested by disconnecting the ergometer cable and moving the actuator rod to its minimum position. A serial command that changes the position reference from 0 to a set value (in degree) is sent. The test was completed nine times, three times going from 0 to 10 degrees, three from 0 to 20 degrees, and three more going from 0 to 40 degrees. Figure 32 shows the step response of three averaged test sets.

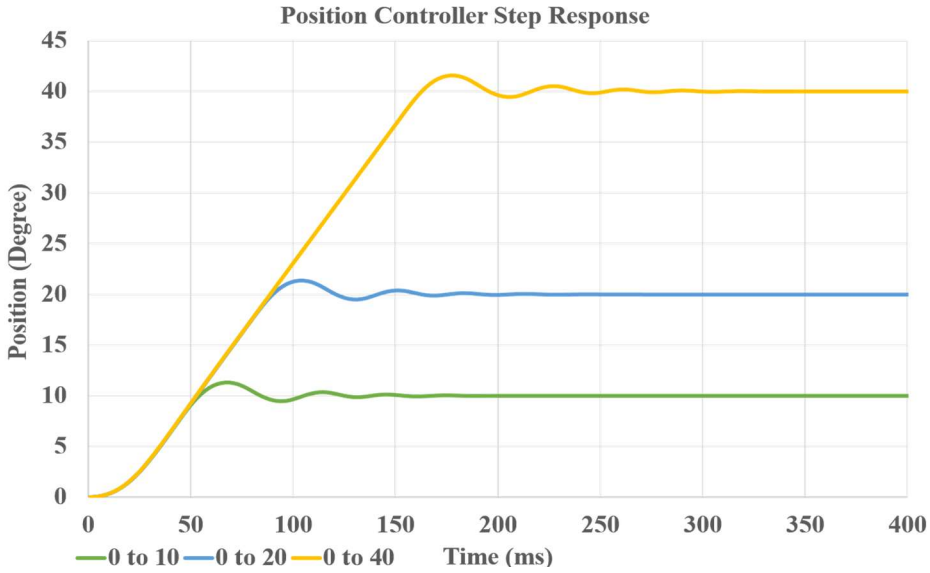

Figure 32: Position Controller Step Response

The step response data were analyzed and the rising time (10 to 90%), the settling time (2% of reference), the percent overshoot, and the integral absolute errors were calculated. The results are summarized in Table 3. The controller is underdamped; however, it still settles quickly. The integral absolute error is very low which is expected when no load is applied.

	Rise Time (ms)	Settling Time (ms)	% Overshoot	Integral Absolute Error (Degree)
0 to 10	33.19±0.062	119.78±0.89	13.2±0.1	0.617±0.178 E-2
0 to 20	59.15±0.045	146.08±10.16	6.9±0.025	0.636±0.153 E-2
0 to 40	116.25±0.012	187.91±0.502	3.95±0.025	1.923±0.0859 E-2

Table 3: Position Controller Evaluation Summary

5.2 Velocity Controller Performance Evaluation

The test was carried out with the actuator disconnected from the ergometer to evaluate the velocity controller. The actuator was moved to the minimum position, and the reference value for the velocity was changed from 0 to a set value. The test was completed nine times (three from 0 to 50 deg/s, three from 0 to 100 deg/s, and three from 0 to 200 deg/s). Figure 32 shows the velocity step response of three averaged test sets.

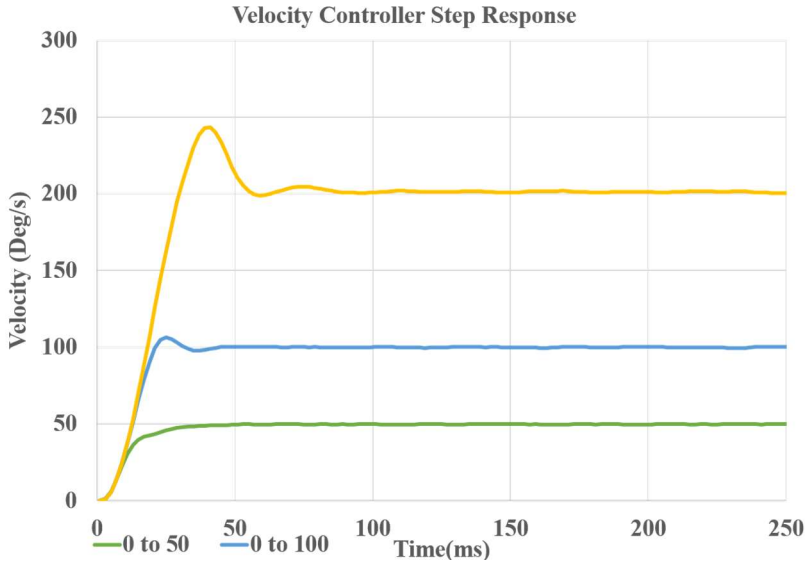

Figure 33: Velocity Controller Step Response

The rising time (10 to 90%), the settling time (2% of reference), the percent overshoot, and the integral absolute errors were calculated using the step response data. The results of the analysis are summarized in Table 4. The performance of the controller changed significantly at different reference values. The system went from being overdamped in the 0 to 50 tests with a very low overshoot value to being underdamped with a much higher overshoot in the other tests. However, the controller remained stable and settled quickly in all tests.

	Rise Time (ms)	Settling Time (ms)	% Overshoot	Integral Absolute Error (Deg/s)
0 to 50	18.85±0.49	40.90±3.41	0.327±0.053	0.115±0.017
0 to100	12.68±0.162	36.38±4.12	6.31±0.32	0.167±0.0114
0 to 200	18.84±0.054	70.87±9.78	21.83±0.198	0.676±0.0127

Table 4: Velocity Controller Evaluation Summary

5.3 Torque Controller Performance Evaluation

The torque controller was tested with the cable attached to the ergometer. To maintain tension in the cable, each test started with an initial torque value of 5 Nm for all but the 100 Nm step test, which started at 50Nm. Nine tests were done; three from 5 to 25 Nm, three from 5 to 50 Nm, and a set of three from 50 to 100 Nm. Figure 34 shows the torque step response of three averaged test sets.

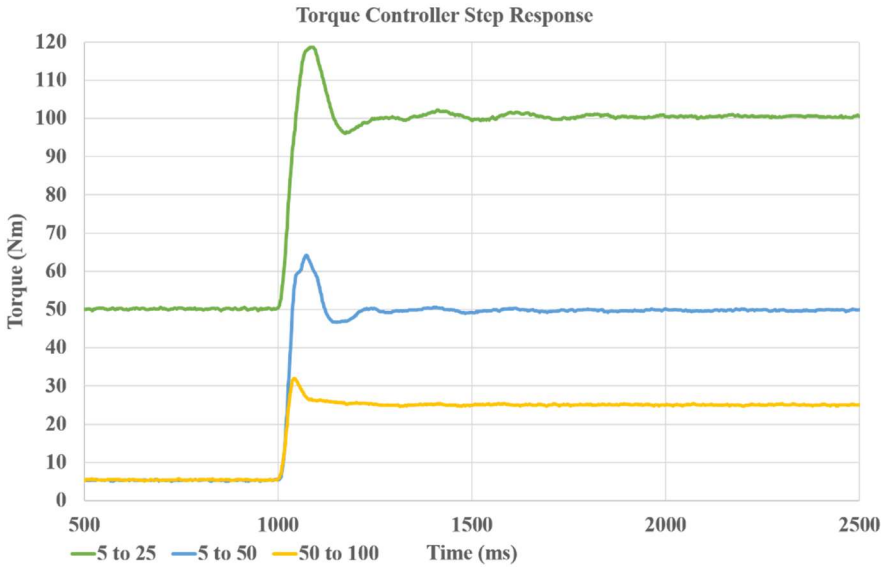

Figure 34: Torque Controller Step Response

Step response data were shifted by the initial torque value. The rising time (10 to 90%), the settling time (5% of reference), the percent overshoot, and the integral absolute errors were calculated using the step response data. The results of the analysis are summarized in Table 5. Unlike the other two controllers, the torque controller changes its gains based on the reference to maintain stability. The controller has a slower response compared to the speed controller, which is why the speed controller is used to maintain power in the constant power mode.

	Rise Time (ms)	Settling Time (ms)	% Overshoot	Integral Absolute Error (Nm)
5 to 25	18.75±2.03	132.92±9.75	37.64±2.40	1.38±0.22
5 to 50	21.55±0.42	191.3±8.57	31.86±0.81	1.57±0.052
50 to 100	30.55±1.21	198.48±7.87	37.7±0.14	2.74±0.06

Table 5: Torque Controller Evaluation Summary

5.4 Validating the Isometric Mode Controller

The stiffness of the controller is the main property to test in isometric mode. An ideal isometric test will not move at all at any applied load. To test the stiffness, the ergometer was mounted in place and attached to the actuator using a cable. A participant was strapped in place with the ergometer at the correct height setting, and three isometric maximum voluntary contractions were performed. Position and torque data were recorded at 500 Hz. The data are used to plot the position versus torque curves in Figure 35.

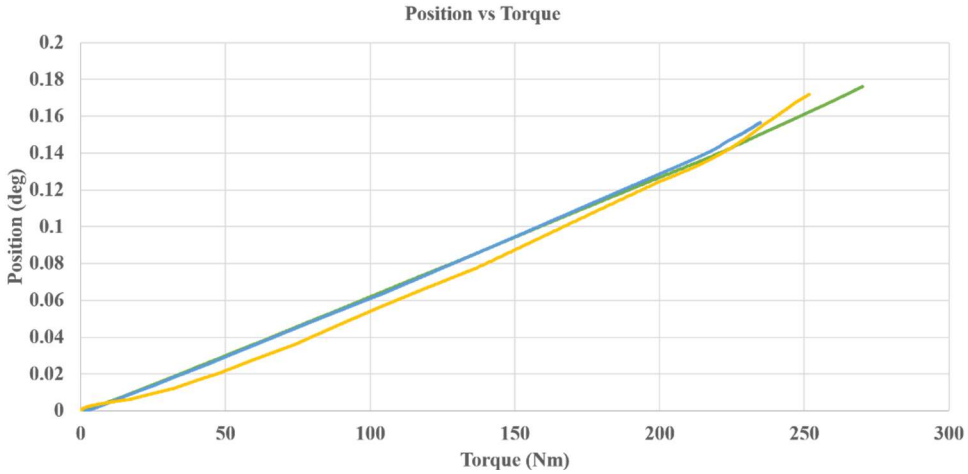

Figure 35: Isometric Mode Torque vs Position

Using linear curve fitting, the stiffness of the controller was calculated at 1506±20 Nm/deg. Figure 36 shows a plot of torque and position vs time during an isometric contraction.

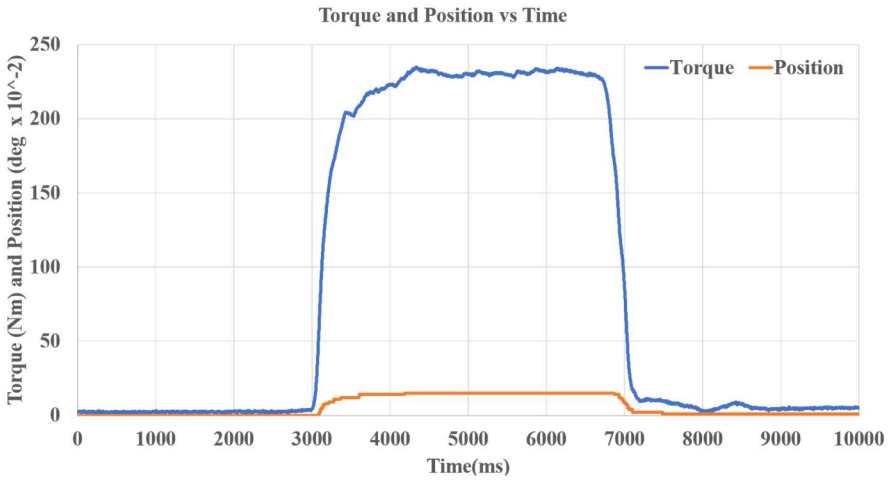

Figure 36: Isotonic Contraction

5.5 Validating the Isotonic Mode Controller

The parameters to check for in the isotonic mode are the maximum percent overshoot and mean percent error during the contraction, excluding the isometric portion. Rise and settling time take significantly longer in this mode since the reference value is filtered at 4 Hz to insure stability. An ideal isotonic controller would have a 0% maximum overshoot and a 0% error.

The Isotonic mode was tested with the ergometer locked in place and attached to the linear actuator via a cable. The torque applied was set to 50 Nm then to 100 Nm, and three isotonic contractions were performed at each reference value. Data were collected at 500 Hz. Figures 37 and 38 shows a plot of torque and position for three isotonic contractions at 50 and 100 Nm respectively.

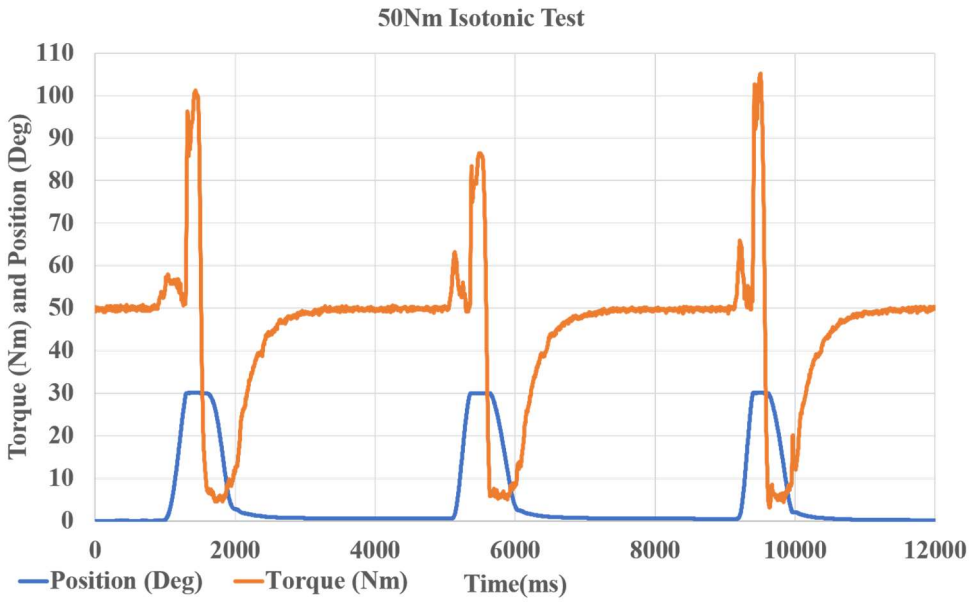

Figure 37: Three 50Nm Isotonic Contractions

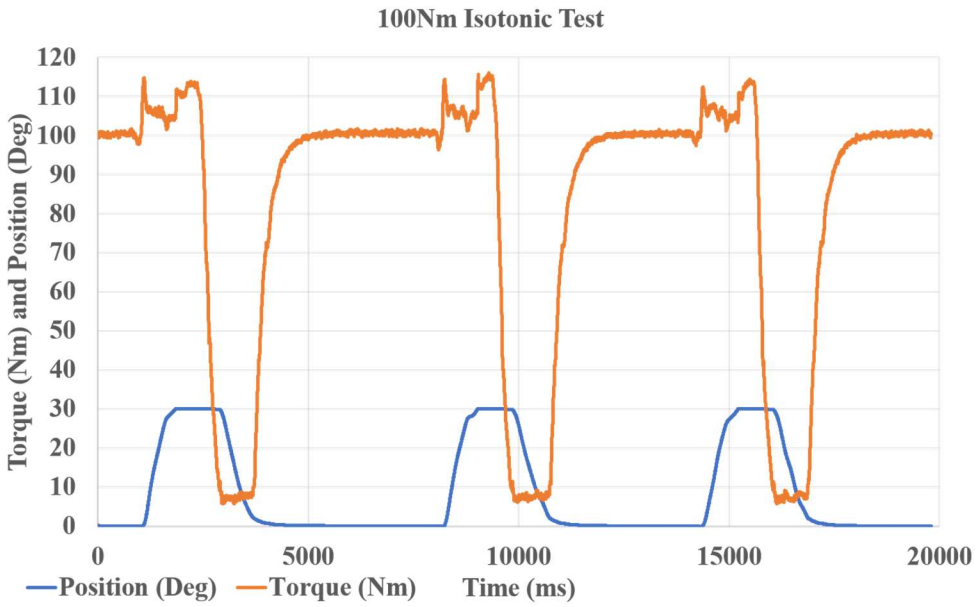

Figure 38: Three 100Nm Isotonic Contractions

The maximum percent overshoot was 24.75±6.67% for the 50 Nm test and 13.87±0.853% for the 100 Nm test. The mean percent error was 7.58±0.55% for the 50 Nm test and 4.58±0.85% for the 100 Nm test. The result shows that the actual maximum overshoot mean error values did not change by much between the two tests, which meant that the percentages about doubled for the 50 Nm one. The error is likely caused by a delay in the controller's response to a rapid change in torque, which happens at the start of each contraction. Which indicates that the percentage error value will be lower at higher torque reference values.

5.6 Validating the Isokinetic Mode Controller

The maximum percent overshoot and mean percent error during the contraction are the main performance metrics here. Rise and settling time are dependent on the participant's contraction speed. This mode was tested with the ergometer set to the correct height setting, locked in place and attached to the linear actuator via a cable. A participant was strapped to the ergometer and performed multiple isokinetic contractions. The speed limit was set to 50, 100 and 150 deg/s for three contractions each while data were sampled at 500 Hz. Figure 39, 40 and 41 show three isokinetic contraction plots at 50 100 and 150 deg/s respectively.

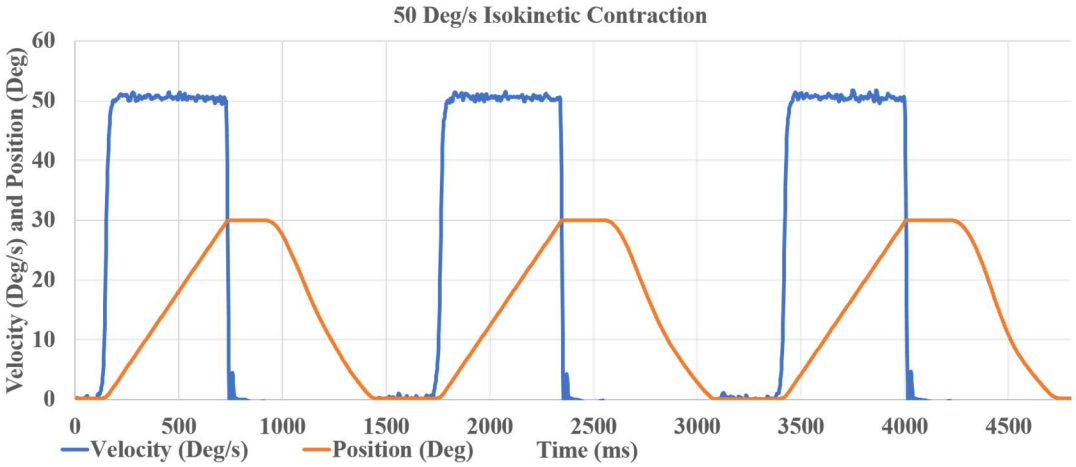

Figure 39: Three Isokinetic Contraction with a 50 Deg/s Velocity Limit

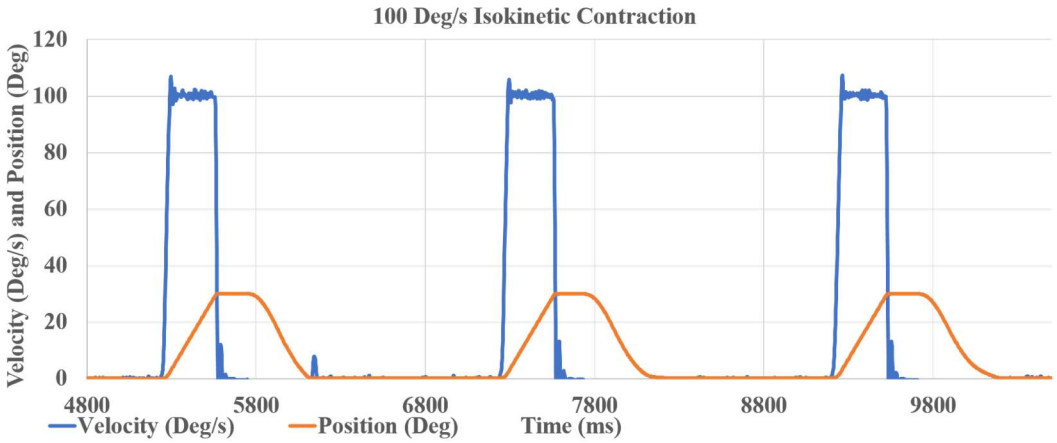

Figure 40: Three Isokinetic Contraction with a 100 Deg/s Velocity Limit

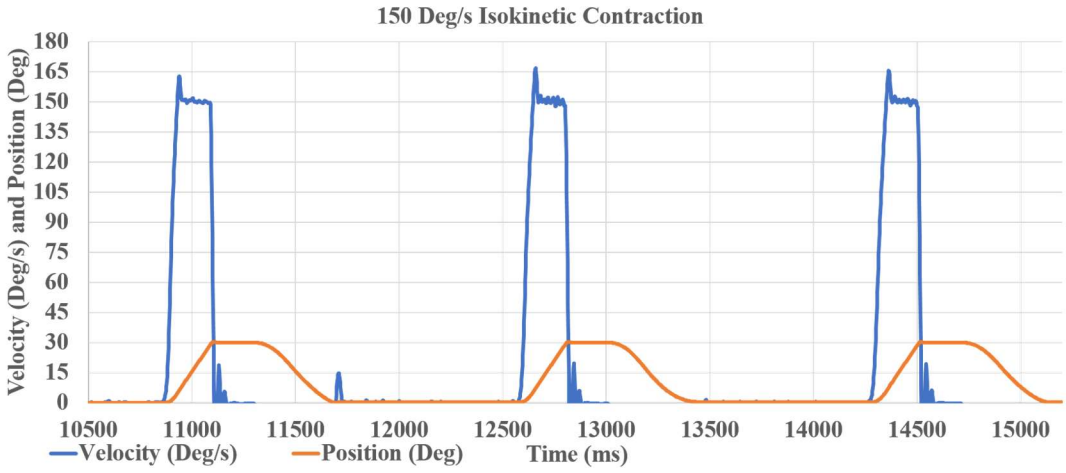

Figure 41: Three Isokinetic Contraction with a 150 Deg/s Velocity Limit

The maximum percent overshoot and mean percent error values during the isokinetic phase of the contraction were calculated using the test data. The results are summarized in Table 6. The maximum percent overshoot value is close to those of the velocity controller with no load which indicates that the controller has high stiffness.

	50 Deg/s Limit	100 Deg/s Limit	150 Deg/s Limit
Mean % Error	1.211±0.078	0.096±0.34	1.014±0.15
Max % Overshoot	3.23±0.37	4.99±1.88	10.03±1.13

Table 6: Isokinetic Controller Evaluation Parameters

5.7 Validating Constant Power Mode Controller

The maximum percent overshoot and mean percent error are also the main two parameters used to evaluate the performance of the constant power controller. The rise time (10 to 90%) is also used for evaluation since the controller is in control of the contraction speed once the torque threshold is reached. The constant power mode was tested with the ergometer locked in place and attached to the linear actuator via a cable. The power reference was set to 50 W for the first three contractions, then switched to 100 W followed by 150 W for three contractions each. Data were collected at 500 Hz, and the power was calculated using the velocity and torque readings. Figure 42 shows how the velocity changes based on torque to maintain power at 50 W.

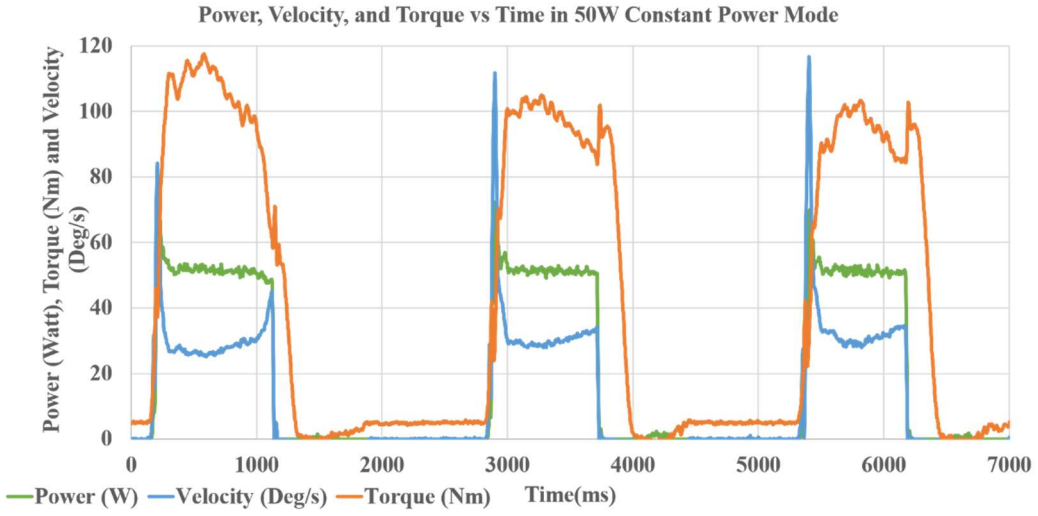

Figure 42: Constant Power Mode Velocity and Torque Relation

Figures 43, 44 and 45 show three constant power contraction plots of position and power at 50 100 and 150 W reference, respectively.

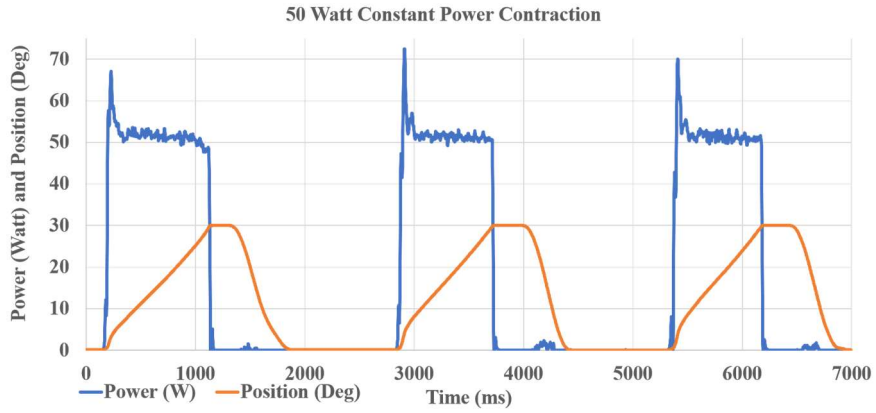

Figure 43: Three Constant Power Contractions with a 50 Watt reference

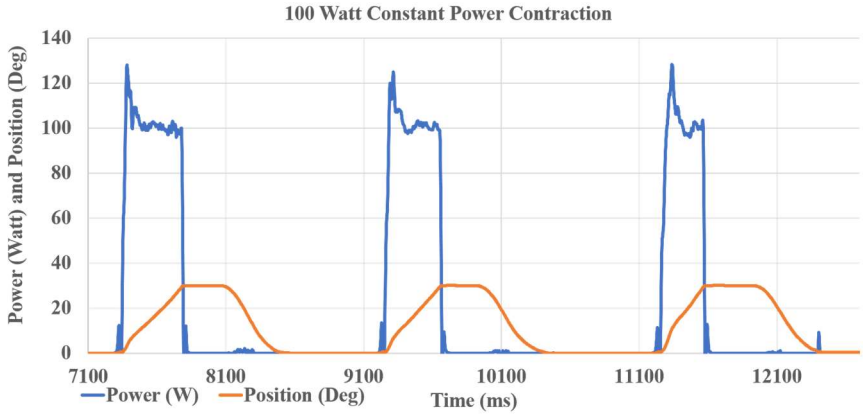

Figure 44: Three Constant Power Contractions with a 100 Watt reference

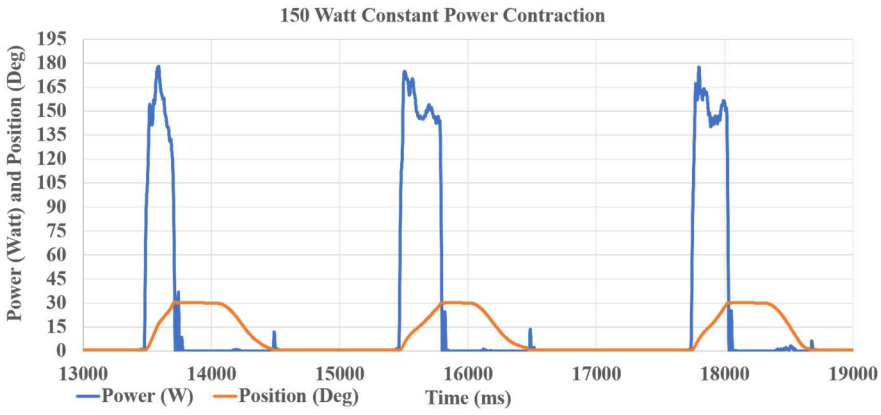

Figure 45: Three Constant Power Contractions with a 150 Watt reference

The rising time, maximum percent overshoot, and mean percent error values during the constant power phase of the contraction were calculated using the test data. The results are summarized in Table 7. The constant power controller performance is closely related to the way the speed controller is tuned. The rising time is longer but comparable to that of the speed controller with no load at 100 deg/s (close to the initial 2 rad/s velocity). The mean percent error value shows that the controller stays close to the reference overall even though it overshoots significantly at the start of each contraction.

	50 Watt	100 Watt	150 Watt
Rising Time (ms)	32.9±15.1	54.65±6.12	25.58±4.622
Max % Overshoot	39.78±5.21	27.02±1.14	17.88±0.83
Mean % Error	3.92±0.2661	3.49±0.73	8.07±1.74

Table 7: Constant Power Controller Evaluation Parameters

5.8 Prolonged System Trial: A Four Minute Isokinetic Fatigue Test

The ergometer was mounted inside the scanner, and a participant was strapped in place with the ergometer at the correct height setting. The audiovisual feedback system was turned on, and the protocol was configured using the user interface. 120 isokinetic contraction with a delay of 2 seconds between each were performed. The velocity limit was set to 240 deg/s. Position, velocity, and torque data were recorded at 500Hz. Figures 45, 46, 47, and 48 show the peak power, velocity, torque and energy used for each contraction respectively.

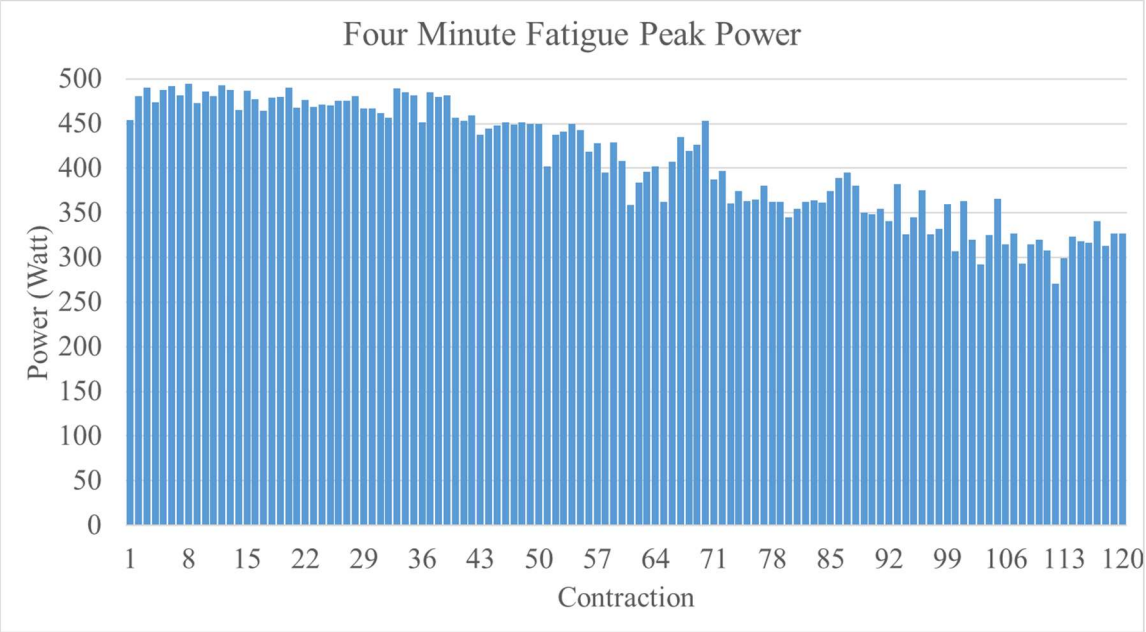

Figure 46: Peak Power Bar Plot

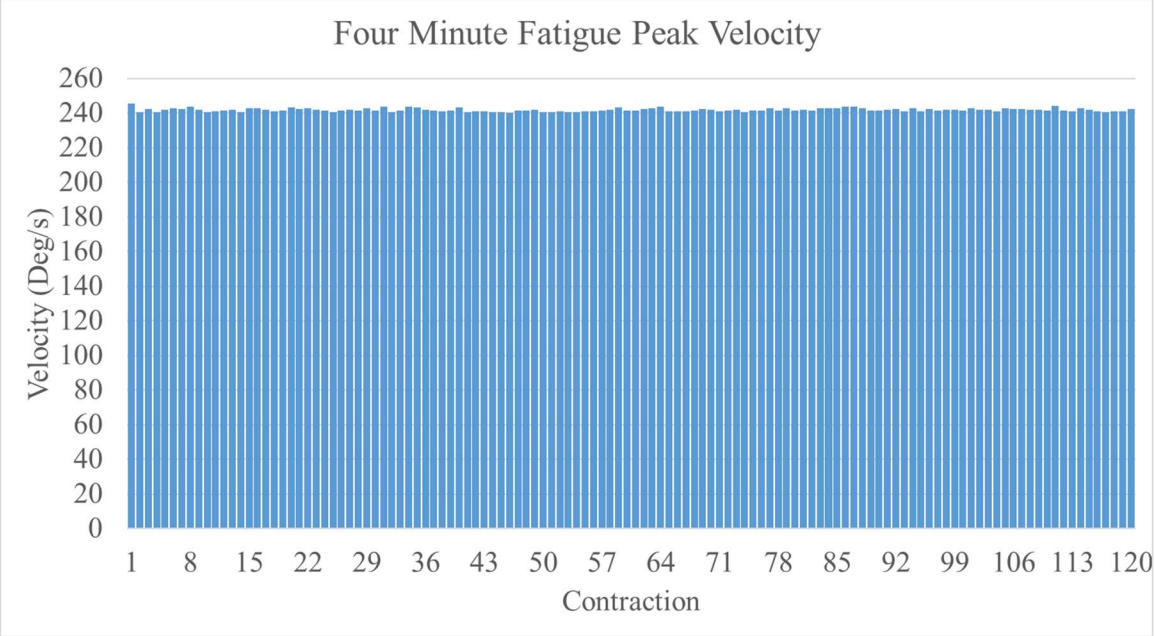

Figure 47: Peak Velocity Bar Plot

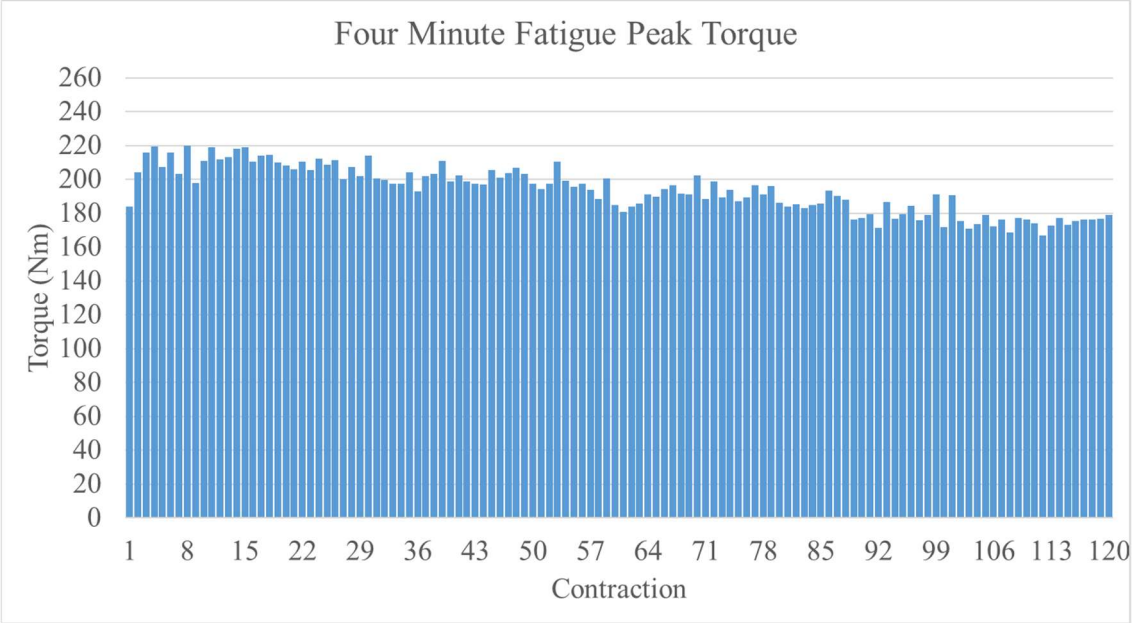

Figure 48: Peak Torque Bar Plot

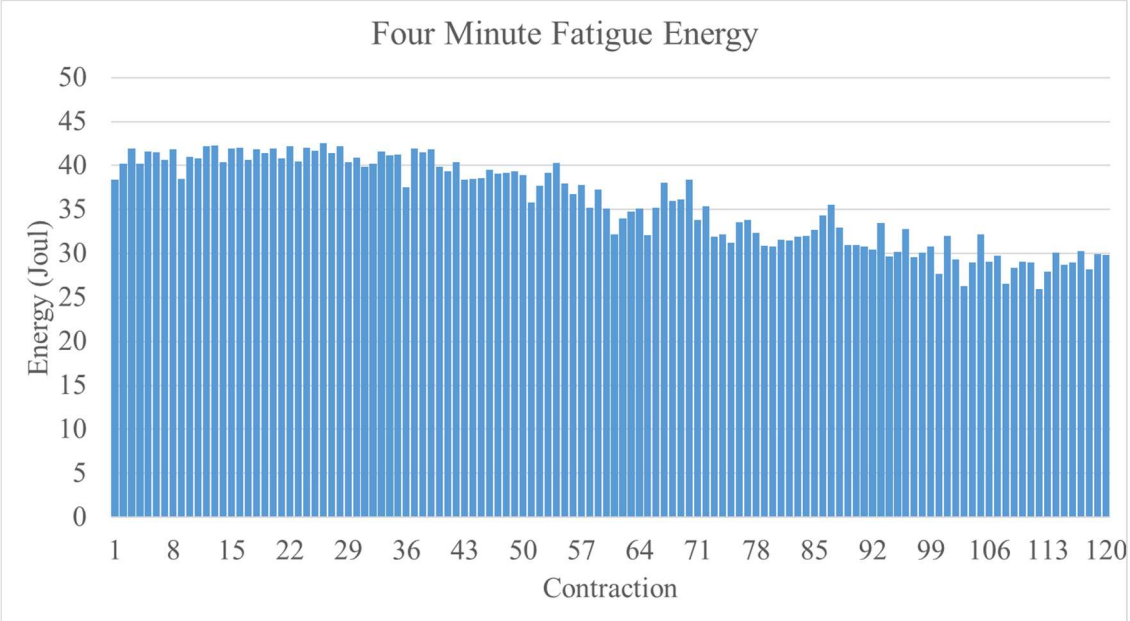

Figure 49: Energy Bar Plot

The peak velocity reading averaged 241.8 deg/s, very close to the 240 deg/s limit. The percent drop in power, torque, and energy were 55%, 76% and 61% respectively, indicating that the participant did fatigue after 4 minutes of exercise.

CHAPTER 6

CONCLUSION

Magnetic resonance imaging and spectroscopy can be used to noninvasively measure the metabolic energy of active muscles, which can be compared to the work measured mechanically. This requires an ergometer; an exercising machine capable of measuring and controlling the resistive load it produces. However, due to the extreme electromagnetic conditions inside a magnetic resonance machine, the design process should take multiple nonstandard considerations into account. Those include both the effects of the device to be designed to the scanning quality and the effect of the scanner fields on the device and its performance.

The ergometer described in this work aims to target muscle groups in the lower limb, enabling static and dynamic muscle contraction types. This is achieved by combining a passive, electromagnetically safe mechanism inside the magnet and an AC servo actuator in another room. The two parts are connected by a cable passing through a system of pulleys. The system can be used to study the biochemical dynamics and physical activation of the muscles during constant static (isometric) contraction, constant load, variable speed (isotonic) contraction, and limited speed, variable loading (isokinetic) contraction. It also allows for a contraction that has a constant power output through its range. The device was designed to be easily adapted to produce the resistive load linearly, allowing the study of the lower limb muscle groups while performing full leg extension. In its linear mode, the device can also be used to apply high forces on soft tissue. This can be combined with magnetic resonance imaging to accurately study the deformation of that tissue and estimate its material properties. Due to the flexibility of the mounting system, the position of the device in the bore can be changed by changing two PVC rods. A placement close to the back of the magnet can allow the user's chest to be near the isocenter enabling cardiovascular assessment under controlled load conditions [32]. If the ergometer was mounted further back, fMRI studies about the effect of exercise on brain activity could be done [23].

REFERENCES

[1]: Ningbo Yu, Roger Gassert, Robert Riener. “Mutual interferences and design principles for mechatronic devices in magnetic resonance imaging”. Int J CARS (2011) 6:473-488.

[2]: Kristen Coyne. “MRI: A Guided Tour”. MagLab. <https://nationalmaglab.org/education/magnet-academy/learn-the-basics/stories/mri-a-guided-tour> January 2015.

[3]: Perry Sprawls. “Magnetic Resonance Imaging: Principles, Methods, and Techniques.” Medical Physics Publishing (2000) ISBN 9780944838976.

[4]: Stefan Blüml. “Magnetic Resonance Spectroscopy: Basics” Chapter 2 from the book “MR Spectroscopy of Pediatric Brain Disorders”, 11 DOI 10.1007/978-1-4419-5864-8_2.

[5] Nikolaos V. Tsekos, Azadeh Khanicheh, Eftychios Christoforou, Constantinos Mavroidis. “Magnetic Resonance– Compatible Robotic and Mechatronics Systems for Image-Guided Interventions and Rehabilitation: A Review Study”. Annu. Rev. Biomed. Eng. 2007. 9:351–87

[6] Beth A. Schueler, PhD, Todd B. Parrish, PhD, Jyh-Cherng Lin, Bruce E. Hammer, Brian J. Pangrle, E. Russell Ritenour, John Kucharczyk, Charles L. Truwit. “MRI Compatibility and Visibility Assessment of Implantable Medical Devices”. JOURNAL OF MAGNETIC RESONANCE IMAGING 9:596–603 (1999).

[7] Chinzei K, Kikinis R, Jolesz FA. “MR compatibility of mechatronic devices: design criteria”. The international conference on medical image computing and computer-assisted intervention Computer Assisted Intervention, pp. 1020–31. Cambridge, UK, 1999.

[8] Schenck JF. “MR Safety at High Magnetic Fields“. Magn Reson Imaging Clin N Am. 1998 Nov;6(4):715-30.

[9] PA Patient Safety Authority. “Safety in the MR Environment: Ferromagnetic Projectile Objects in the MRI Scanner Room” Pa Patient Saf Advis 2009 Jun;6(2):56-62.

[10] Shellock FG. “Radiofrequency energy-induced heating during MR procedures: a review.” Journal of Magnetic Resonance Imaging 12:30–36, 2000.

[11] Schenck JF. “The role of magnetic susceptibility in magnetic resonance imaging: MRI magnetic compatibility of the first and second kinds” Med Phys. 1996 Jun;23(6):815-50.

[12] Nikolaos V., Tsekos, Eftychios Christoforou, Alpay Ozcan. “A General-Purpose MR-Compatible Robotic System: Implementation and Image Guidance for Performing Minimally Invasive Interventions”. IEEE Eng Med Biol Mag. 2008 ; 27(3): 51–58.

[13] Tsekos NV, Ozcan A, Christoforou E. “A Prototype Manipulator for MR Guided Interventions Inside Standard Cylindrical MRI Scanners” Journal of Biomechanical Engineering 127:972–80.

[14] Chinzei K, Hata N, Jolesz F, Kikinis R. “MR compatible surgical assist robot: system integration and preliminary feasibility study”. Proc. Med. Image Comput. Comput.-Assisted Intervention, pp. 921–30. Pittsburgh, PA: Springer 2000.

[15] Ming Li, Dumitru Mazilu, Keith A. Horvath. “Robotic System for Transapical Aortic Valve Replacement with MRI Guidance”. Med Image Comput Comput Assist Interv. 2008; 11(Pt 2): 476–484.

[16] U-Xuan Tan, Bo Yang, Rao Gullapalli, Jaydev P. Desai. “Tri-Axial MRI Compatible Fiber-optic Force Sensor” IEEE Trans Robot. 2011 February 1; 27(1): 65–74.

[17] Gassert R, Moser R, Burdet E, Bleuler H. “MRI/fMRI-Compatible Robotic System with Force Feedback for Interaction with Human Motion”. IEEE/ASME TRANSACTIONS ON MECHATRONICS, VOL. 11, NO. 2, APRIL 2006

[18] N. Takahashi, M. Tada, J. Ueda, Y. Matsumoto, T. Ogasawara. “An Optical 6-axis Force Sensor for Brain Function Analysis using fMRI”. Proc. IEEE Int. Conf. Sensors, pp. 253–58, Toronto, Canada

[19]: Su H, Shang W, Cole GA, Li G, Harrington K, Camilo A, Tokuda J, Tempany CM, Hata N, Fischer GS. “Piezoelectrically Actuated Robotic System for MRI-Guided Prostate Percutaneous Therapy”. IEEE/ASME Transactions on Mechatronics, Vol 20, No 4, Aug 2015.

[20] Gregory Cole, Julie Pilitsis, and Gregory S. Fischer. “Design of a Robotic System for MRI-Guided Deep Brain Stimulation Electrode Placement” 2009 IEEE International Conference on Robotics and Automation, Kobe, Japan, May 12-17, 2009.

[21] Moser R, Gassert R, Burdet E, Sache L, Woodtli HR. “An MR compatible robot technology” Proc. IEEE Int. Conf. Robotics Automation, pp. 670– 75, Taipei, Taiwan 2003.

[22] Dan Stoianovici, Alexandru Patriciu, Doru Petrisor, Dumitru Mazilu, Louis Kavoussi. “A New Type of Motor: Pneumatic Step Motor”. IEEE/ASME TRANSACTIONS ON MECHATRONICS, VOL. 12, NO. 1, FEBRUARY 2007

[23] Eduardo B Fontes, Alexandre H Okano, François De Guio, Elske J Schabort, Li Li Min, Fabien A Basset, Dan J Stein, Timothy D Noakes. “Brain Activity and Perceived Exertion During Cycling Exercise: An fMRI Study” BJSM Online 10.1136/bjsports-2012-091924

[24] Ryschon TW, Fowler MD, Arai AA, Wysong RE, Leighton SB, Clem TR Sr, Balaban RS. “A Multimode Dynamometer for in Vivo MRS Studies of Human Skeletal Muscle”. J Appl Physiol (1985). 1995 Dec;79(6):2139-47.

[25] Bangsbo J, Johansen L, Quistorff B, Saltin B. “NMR and analytical biochemical evaluation of CrP and nucleotides in the human calf during muscle contraction”. J Appl Physiol 1993;74:2034–2039.

[26] Miller RG, Boska MD, Moussavi RS, Carson PJ, Weiner MW. “31Pnuclear magnetic resonance studies of high energy phosphates and pH in human muscle fatigue: comparison of aerobic and anaerobic exercise” J Clin Invest 1988;81:1190–1196.

[27] Maria Pia Francescato, Valentina Cettolo. “Two-Pedal Ergometer for In Vivo MRS Studies of Human Calf Muscles”. Magnetic Resonance in Medicine 46:1000–1005 (2001).

[28] Quistorff, B., Nielsen, S., Thomsen, C., Jensen, K. E., & Henriksen, O. “A simple calf muscle ergometer for use in a standard whole-body MR scanner”. Magnetic Resonance in Medicine, 13(3), 444-449 1990

[29] Smith SA, Montain SJ, Matott RP, Zientara GP, Jolesz FA, Fielding RA. “Creatine supplementation and age influence muscle metabolism during exercise”. J Appl Physiol (1985). 1998 Oct;85(4):1349-56.

[30] Gwenael Layec, Aurélien Bringard, Christophe Vilmen, Jean-Paul Micallef, Yann Le Fur, Stéphane Perrey, Patrick J. Cozzone, David Bendahan. “Accurate work-rate measurements during in vivo MRS studies of exercising human quadriceps” Magn Reson Mater Phy (2008) 21:227–235.

[31] Yoshida T1, Watari H, Tagawa K. “Effects of active and passive recoveries on splitting of the inorganic phosphate peak determined by 31P-nuclear magnetic resonance spectroscopy” NMR Biomed. 1996 Feb;9(1):13-9.

[32] Silmara Gusso1, Carlo Salvador, Paul Hofman, Wayne Cutfield, James C Baldi, Andrew Taberner, Poul Nielse “Design and testing of an MRI-compatible cycle ergometer for non-invasive cardiac assessments during exercise” Gusso et al. BioMedical Engineering OnLine 2012, 11:13.

[33] National Center for Health Statistics “Data Table of Stature-for-age Charts”. Center for Disease Control and Prevention <http://www.cdc.gov/growthcharts/html_charts/statage.htm>

[34] John Hawks. “Predicting stature from bone measurements” john hawks weblog Sep 2011.

[35] Izzet Duyar, Can Pelin. “Body Height Estimation Based on Tibia Length in Different Stature Groups”. American Journal of Physical Anthropology 122:23–27 (2003).

[36] Doug Ito, Ian Beavers. “When 1 + 1 = +3 (dB): Averaging ADC Channels to Improve NSD”. ElectronicDesign.com < http://electronicdesign.com/analog/when-1-1-3-db-averaging-adc-channels-improve-nsd> October 2015

[37] Ryota Shimose, Nobuyuki Ushigome, Chigaya Tadano, Hitoshi Sugawara, Masae Yona, Atsuhiko Matsunaga, Masuo Muro. “Increase in rate of force development with skin cooling during isometric knee extension” Journal of Electromyography and Kinesiology 24 (2014) 895–901.

[38] Helen L Schimidt, Álvaro S Machado, Marco A Vaz, Felipe P Carpes. “Isometric muscle force, rate of force development and knee extensor neuromuscular efficiency asymmetries at different age groups” Rev Bras Cineantropom Desempenho Hum 2014, 16(3):307-315.